

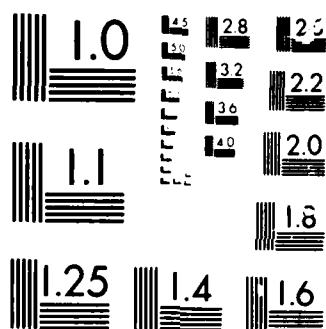
NEW ULTRA LOW PERMITTIVITY COMPOSITES FOR USE IN  
CERAMIC PACKAGING OF GA:.. (U) PENNSYLVANIA STATE UNIV  
UNIVERSITY PARK MATERIALS RESEARCH LAB. L E CROSS

**UNCLASSIFIED**

18 SEP 85 N00014-84-K-0721

F/G 9/5

NL



5

AD-A168 877

NEW ULTRA LOW PERMITTIVITY COMPOSITES FOR USE IN CERAMIC  
PACKAGING OF Ga:As INTEGRATED CIRCUITS

Annual Report  
August 1, 1984 to July 31, 1985

ONR Contract N00014-84 K-0721

DARPA Order No. 5157

September 18, 1985

DTIC FILE COPY

NOTED  
10/1/85  
10/1/85  
10/1/85

DTIC  
ELECTE  
JUN 20 1986  
S D E



**THE MATERIALS RESEARCH LABORATORY**  
THE PENNSYLVANIA STATE UNIVERSITY  
UNIVERSITY PARK, PENNSYLVANIA

## REPORT DOCUMENTATION PAGE

1a. REPORT SECURITY CLASSIFICATION Unclassified			1b. RESTRICTIVE MARKINGS		
2a. SECURITY CLASSIFICATION AUTHORITY			3. DISTRIBUTION/AVAILABILITY OF REPORT		
2b. DECLASSIFICATION/DOWNGRADING SCHEDULE					
4. PERFORMING ORGANIZATION REPORT NUMBER(S)			5. MONITORING ORGANIZATION REPORT NUMBER(S)		
6a. NAME OF PERFORMING ORGANIZATION The Pennsylvania State Univ. Materials Research Laboratory		6b. OFFICE SYMBOL (If applicable)	7a. NAME OF MONITORING ORGANIZATION /		
6c. ADDRESS (City, State and ZIP Code) Materials Research Laboratory The Pennsylvania State University University Park, PA 16802			7b. ADDRESS (City, State and ZIP Code)		
8a. NAME OF FUNDING/SPONSORING ORGANIZATION Office of Naval Research		8b. OFFICE SYMBOL (If applicable)	9. PROCUREMENT INSTRUMENT IDENTIFICATION NUMBER —		
8c. ADDRESS (City, State and ZIP Code) Ballston Tower 800 N. Quincy Street Arlington, VA 22217			10. SOURCE OF FUNDING NOS.		
11. TITLE (Include Security Classification) New Ultra Low Permittivity Composites for Use in ...			PROGRAM ELEMENT NO.	PROJECT NO.	TASK NO.
12. PERSONAL AUTHOR(S) L.E. Cross			WORK UNIT NO.		
13a. TYPE OF REPORT Annual Report	13b. TIME COVERED FROM 8/1/84 TO 7/31/85	14. DATE OF REPORT (Yr., Mo., Day) September 18, 1985	15. PAGE COUNT 65		
16. SUPPLEMENTARY NOTATION					
17. COSATI CODES			18. SUBJECT TERMS (Continue on reverse if necessary and identify by block number)		
FIELD	GROUP	SUB. GR.			
19. ABSTRACT (Continue on reverse if necessary and identify by block number)					
<p>This report documents work performed over the first year of a new three-year joint program between the Materials Research Laboratory at Penn State and Interamics Co. in La Jolla, California, to develop materials systems for use in the ceramic packaging of Ga:As integrated circuits. The period covered is from August 1, 1984, to July 31, 1985. Topics under study at Penn State are: dielectrics produced from Macro-Defect-Free (MDF) cements. Both aluminate and silicate based cements have been studied. The objectives of the first year's work have been to show that suitable test tablets can be produced which exhibit dielectric losses less than 1% into the frequency range of 2.5 GHz. Current work is focused upon lowering the permittivity level using silica microballoons dispersed in the matrix.</p> <p>Sol-gel preparation of both thick (25 <math>\mu</math>) and thin (0.5 <math>\mu</math>) SiO<sub>2</sub> and silica:alumina films has shown that in the diphasic system, it is possible to produce crack-free monoliths with</p>					
20. DISTRIBUTION/AVAILABILITY OF ABSTRACT UNCLASSIFIED/UNLIMITED <input type="checkbox"/> SAME AS RPT. <input type="checkbox"/> DTIC USERS <input type="checkbox"/>			21. ABSTRACT SECURITY CLASSIFICATION		
22a. NAME OF RESPONSIBLE INDIVIDUAL		22b. TELEPHONE NUMBER (Include Area Code)		22c. OFFICE SYMBOL	

permittivities in the range 1.6 to 2.0 and loss tangents below .003. In the thin films, capping of columnar sputtered:etched films has been demonstrated.

For etched Schott and Vycor glass structures, permittivities in the range 2.5 to 3.0 have been measured with excellent low loss properties. In the microporous Vycor evaporated electrode patterns have been used, and the low loss is preserved into the microwave region.

Sputtered silicon films have been successfully etched to yield highly planar columnar structures up to 25  $\mu$ meters thick. Experiments are in progress to convert the silicon to  $\text{SiO}_2$  by an oxidation step and capping of the columnar structure using sol-gel coatings has been achieved.

In a parallel program at Interamics, new families of borosilicate glass bonded alumina ceramics are being developed. Tapes using both lead and calcium borosilicate glasses have been fabricated and densified at firing temperatures below  $1,000^\circ\text{C}$ . Current studies are exploring suitable metallization techniques.

Accession For	
NTIS GRA&I	<input checked="" type="checkbox"/>
DTIC TAB	<input type="checkbox"/>
Unannounced	<input type="checkbox"/>
Justification	<i>per</i>
By	
Distribution/	
Availability Codes	
Dist	Avail and/or Special
<i>A-1</i>	



## TABLE OF CONTENTS

	<u>Page</u>
1.0 INTRODUCTION. . . . .	1
2.0 RATIONALE FOR THE PRESENT APPROACHES. . . . .	2
3.0 GENERAL CONSIDERATIONS IN DIELECTRIC "MIXING" . . . . .	3
3.1 Series Mixing of Two Phases. . . . .	3
3.2 Discrete Spherical Particles of Second Phase . . . . .	5
3.3 Random Mixing. . . . .	7
3.4 Series Mixing. . . . .	7
4.0 MACRO-DEFECT-FREE CEMENTS . . . . .	8
4.1 Introduction . . . . .	8
4.2 Calcium Aluminate Cements. . . . .	9
4.2.1 Characterization of the Precursor Cements . . . . .	9
4.2.1.1 Chemical Composition . . . . .	9
4.2.1.2 Phase Composition. . . . .	11
4.2.1.3 Density. . . . .	11
4.2.1.4 Surface Area . . . . .	11
4.2.1.5 Particle Size Distribution . . . . .	11
4.2.2 Processing Methods. . . . .	11
4.2.2.1 Shear Mixing: General Procedure . . . . .	15
4.2.3 Dielectric Response . . . . .	16
4.2.4 Effects of Additives. . . . .	21
4.2.5 Silicate Cements. . . . .	23
5.0 SOL-GEL PROCESSING. . . . .	24
5.1 Introduction . . . . .	24
5.2 Thick Film Studies . . . . .	26
5.2.1 Introduction. . . . .	26
5.2.2 Experimental. . . . .	27
5.2.3 Diphasic Organic/Inorganic Gels . . . . .	28
5.2.4 Vapor Deposited Diphasic Materials. . . . .	30
5.2.5 Current and Future Work . . . . .	32
5.3 Thin Film Coatings . . . . .	32
5.3.1 Introduction. . . . .	32
5.3.2 Experimental. . . . .	34

6.0	LEACHED DIPHASIC GLASS STRUCTURES . . . . .	35
6.1	Introduction . . . . .	35
6.2	Schott Glasses . . . . .	35
6.3	Corning Vycor Glass. . . . .	36
7.0	SPUTTER DEPOSITED COATINGS. . . . .	39
7.1	Introduction . . . . .	39
7.2	Deposition of Amorphous Silicon. . . . .	41
7.3	Anisotropic Etching. . . . .	44
7.4	Thermal Oxidation. . . . .	46
7.5	Sol-Gel Coating. . . . .	46
7.6	Summary. . . . .	46
8.0	EVOLUTIONARY STUDIES. . . . .	46
8.1	Introduction . . . . .	46
8.2	Approach to the Problem. . . . .	48
8.3	Preliminary Studies. . . . .	49
8.4	Particle-Size Reduction Studies. . . . .	55
8.5	Firing Studies . . . . .	58
8.6	Metallization Studies. . . . .	60

## 1.0 INTRODUCTION

This report documents work performed over the first year of a new three-year joint program between the Materials Research Laboratory at Penn State University and Interamics in La Jolla, CA, to develop new ultra low permittivity composite dielectrics for use in the ceramic packaging of Ga:As integrated circuits. The period covered by this report is August 1, 1984, to July 31, 1985, and the work was supported by ONR Contract N00014-84-K-0721 under DARPA Order No. 5157.

Topics for study during this first year have been; at Penn State

- 1) Dielectrics produced from macro-defect-free cements,
- 2) Sol-gel processing of thick film silicate and diphasic silicate aluminate dielectrics,
- 3) Etched porous glass films,
- 4) Sputter deposited porous film structures.

At Interamics, the objective has been to evolve from the current alumina based dielectrics, towards the lower temperature processing envisaged in the Penn State approaches. As the first step in this process, new borosilicate glass bonded alumina ceramics are under study where it is evident that processing temperatures can be reduced to below 1000°C and are compatible with gold or silver palladium metallization.

In the Penn State program, the sub-tasks are each supervised by a faculty member who is a recognized authority in the materials area under study, the overall program is coordinated by L.E. Cross with the help of Dr. T.R. Gururaja, electrical measurements for all participants are being carried forward on the automated measuring facility under the direction of Paul Moses. Microwave measurements rely mostly upon an HP 8510T measuring system under the direction of Dr. Jin-Hun Kim, assisted by Dr. Sei Joo Jang.



## 2.0 RATIONALE FOR THE PRESENT APPROACHES

To accomplish the strip line structures at the spacing and wiring densities which will be required for the interconnect systems of high speed Ga:As ICs, recent studies by B. Gilbert, et al. at Mayo Clinic, indicate that for dimensions which appear feasible in proposed structures, a basic requirement for the supporting insulator will be an exceedingly low dielectric permittivity. The absolute upper limit which can be tolerated is of order  $3\epsilon_0$  and even lower values would be very highly desirable.

Evaluation of possible inorganic dielectrics indicates a lower limit for single phase materials of order  $3.85 \epsilon_0$  in silica glass, thus it is not possible with existing single phase inorganic dielectrics to achieve this very basic requirement of ultra low permittivity, and a composite approach involving at least one much lower permittivity phase will be essential.

In the approaches taken on this contract, that second phase has been chosen to be gas or vacuum with permittivity  $1 \epsilon_0$ . The focus is then to develop tractable low permittivity inorganic host dielectrics into which a controlled closed pore structure can be introduced by suitable processing. Since any pore structure will necessarily introduce many undesirable "side effects," lowering thermal conductivity, reducing mechanical strength, etc., it is most desirable to control the pore network so as to limit it to regions under the strip line traces, where the consequent permittivity reduction is essential.

Even at the very fast switching rates in the current Ga:As ICs, it is likely that the highest fourier components to be preserved will not go much beyond 30 GHz corresponding to a wavelength in the composite of order 0.7 cm. Clearly this dimension is very much larger than the scale of any of the pore structures being envisaged, so that static effective medium calculation of the average permittivity of the composite can provide an initial guide for

selecting the pore volumes which will be required for any given host permittivity and architecture.

### 3.0 GENERAL CONSIDERATIONS IN DIELECTRIC "MIXING"

The basic approach which is being used for lowering the dielectric permittivity in each of the proposed topics under study is that of "mixing" with the dielectric ceramic pores of controlled geometry which contain an air or inert gas filling and have a relative permittivity close to unity.

A general question which must be addressed is the mode of phase interconnection which can be achieved in the systems under study and the modifications which can be effected to the dielectric properties of the major phase (ceramic dielectric) by these various modes of mixing in the second phase. In general, the sacrifice associated with the introduction of pores is to the mechanical strength and one might wish to use modes of mixing which would keep the volume of the gas phase as small as possible consistent with achieving the needed level of dielectric permittivity in the composite of parent phases under study.

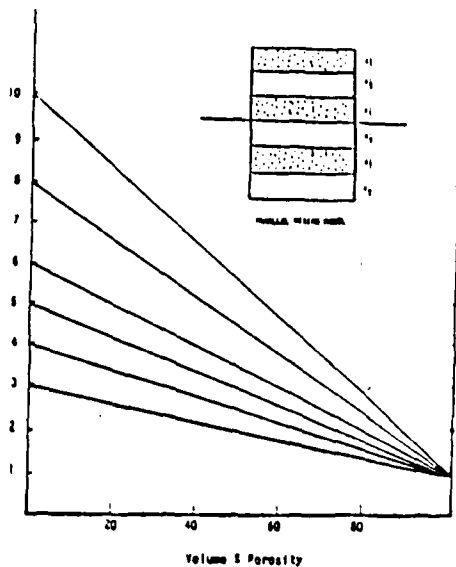
Unfortunately, the general problem of the mixing of two dielectric phases is exceedingly complex, since the manner in which the field is manifested in the composite depends on shape, volume fraction and mode of interconnection between the two phases. However, some simple end member calculations can be a useful guide.

#### 3.1 Series Mixing of Two Phases

For the etched sputtered film structures which are proposed, the dielectric is in the form of a room and pillar structure, with the columns of dielectric dominantly parallel to the electric field direction. This is

Fig. 3.1. Dielectric Mixing Rules.

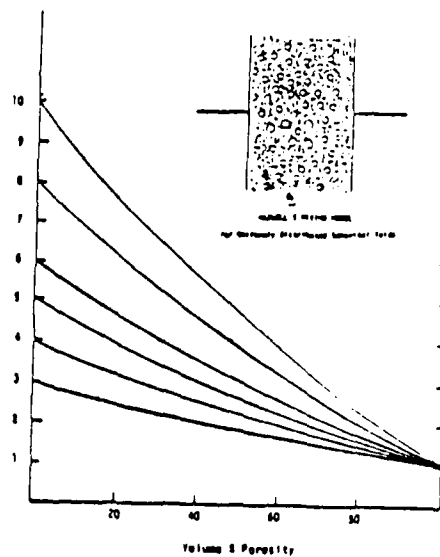
PARALLEL CAPACITIVE MIXING



$$\epsilon' = v_1 \epsilon'_1 + v_2 \epsilon'_2$$

(a)

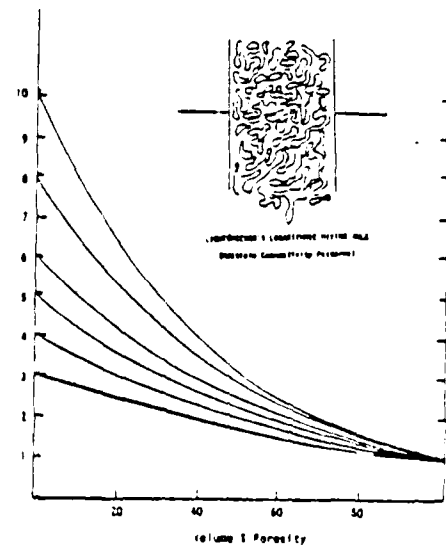
MAXWELL'S MIXING MODEL  
(Spherical, Homogeneously Distributed Pores  
in Continuous Matrix)



$$\epsilon' = \frac{v_2 \epsilon'_2 \left( \frac{2}{3} + \frac{\epsilon'_1}{3\epsilon'_2} \right) + v_1 \epsilon'_1}{v_2 \left( \frac{2}{3} + \frac{\epsilon'_1}{3\epsilon'_2} \right) + v_1}$$

(b)

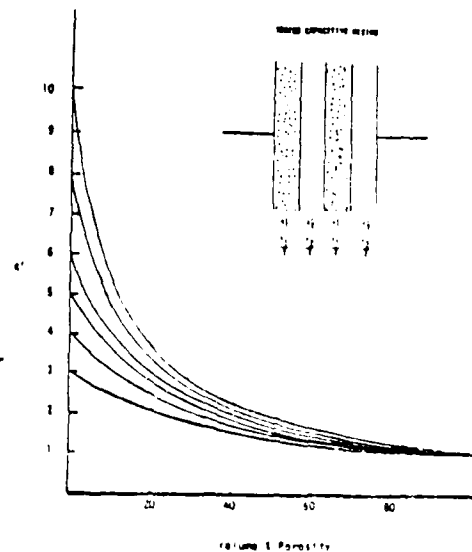
LICHTENHECKER'S LOGARITHMIC MIXING RULE



$$\ln \epsilon' = v_1 \ln \epsilon'_1 + v_2 \ln \epsilon'_2$$

(c)

SERIES CAPACITIVE MIXING



$$\frac{1}{\epsilon'} = \frac{v_1}{\epsilon'_1} + \frac{v_2}{\epsilon'_2}$$

(d)

clearly a case of parallel mixing of the two phases according to Fig. 3.1(a) with

$$\epsilon_{\text{total}} = \sigma_1 \epsilon_1 + \sigma_2 \epsilon_2 \quad 3.1$$

where  $\sigma_1$ ,  $\sigma_2$  are the volume fractions of phases 1 and 2, respectively,  $\epsilon_{\text{total}}$  the resultant mean permittivity  $\epsilon_1$ ,  $\epsilon_2$  the permittivities of phases 1 and 2.

If phase 1 is a gas filled pore structure with  $\epsilon_1 = 1$ ,  $\epsilon_{\text{total}}$  can be calculated from equation 3.1 for a range of values of ceramic phase  $\epsilon_2$  and of volume fraction  $\sigma$  of pores. The results are tabulated in Table 3.1(a) and graphed in Figure 3.1(a). Clearly to achieve an  $\epsilon_{\text{total}} = 3$ , which is our objective at a reasonable pore volume for mechanical strength, it is desirable to have a matrix phase of very low  $\epsilon_1$  and this is the reason for the focus upon  $\text{SiO}_2$  for this part of the program.

### 3.2 Discrete Spherical Particles of Second Phase

The classical model for porosity is one of small spherical pores uniformly distributed in the matrix phase. For this case the Maxwell mixing rule is applicable giving

$$\epsilon_{\text{total}} = \frac{\sigma_2 \epsilon_2 \left( \frac{2}{3} + \frac{\epsilon_1}{3\epsilon_2} \right) + \epsilon_1 \sigma_1}{\sigma_2 \left( \frac{2}{3} + \frac{\epsilon_1}{3\epsilon_2} \right) + \sigma_1} \quad 3.2$$

with gas filled pores  $\epsilon_1 \simeq 1$  and the tabulated data of  $\epsilon_{\text{total}}$  as a function of permittivity of the matrix and volume fraction of pores are given in Table 3.1(b) and Figure 3.1(b).

It is evident that spherical pores are more forgiving so that matrix phase permittivities of 5 to 6 are acceptable as in some of the silicate based MDF cements (Section 4).

Table 3.1. Tabulation of Mixing Rules.

Matrix Permittivity, $\epsilon'$	Volume % Porosity			
	20	40	60	80
3	2.6	2.2	1.8	1.4
4	3.4	2.8	2.2	1.6
5	4.2	3.4	2.6	1.8
6	5.0	4.0	3.0	2.0
8	6.6	5.2	3.8	2.4
10	8.2	6.4	4.6	2.8

Matrix Permittivity, $\epsilon'$	Volume % Porosity			
	20	40	60	80
3	2.51	2.08	1.68	1.33
4	3.25	2.59	2.00	1.47
5	3.98	3.10	2.31	1.62
6	4.71	3.60	2.63	1.76
8	6.17	4.61	3.25	2.05
10	7.63	5.61	3.96	2.34

Maxwell's Mixing Model.

Effects of Parallel Mixing.

Matrix Permittivity, $\epsilon'$	Volume % Porosity			
	20	40	60	80
3	2.41	1.93	1.55	1.25
4	3.03	2.30	1.74	1.32
5	3.62	2.63	1.90	1.38
6	4.19	2.93	2.05	1.43
8	5.28	3.48	2.38	1.52
10	6.31	3.98	2.51	1.58

Matrix Permittivity, $\epsilon'$	Volume % Porosity				
	10	20	40	60	80
3	2.5	2.1	1.7	1.4	1.2
4	3.1	2.5	1.8	1.4	1.2
5	3.6	2.8	1.9	1.5	1.2
6	4.0	3.0	2.0	1.5	1.2
8	4.7	3.3	2.1	1.6	1.2
10	5.3	3.6	2.2	1.6	1.2

Lichtenecker's Mixing Rule.

Tabulations of Series Mixing Parameters.

### 3.3 Random Mixing

For a range of composite dielectrics in which neither parallel nor series mixing is strongly preferred, i.e. systems with random connectivity, the empirical Lichtenecker's logarithmic mixing rule is often applied, i.e.

$$\ln \epsilon_{\text{total}} = \sigma_1 \ln \epsilon_1 + \sigma_2 \ln \epsilon_2 \quad 3.3$$

In the case of interest here with  $\epsilon_1 = 1$ , the data as a function of matrix permittivity and pore volume fraction are given in Table 3.1(c) and graphically in Figure 3.1(c).

Lichtenecker is again a little more favorable but again matrix phase permittivities in the range 5-6 as in the porous glass structures proposed will be necessary to maintain reasonable porosity values.

### 3.4 Series Mixing

For sheet structures in which the  $\epsilon$  field is normal to the sheet, the dielectrics are clearly in series as in Figure 3.1(d), the equivalent circuit is as in Figure 3.1(d). The dielectric permittivity as a function of second phase volume is tabulated in Table 3.1(d) and these data presented graphically in Figure 3.1(d).

The series mode is clearly the most advantageous in reducing permittivity but obviously difficult to realize in a practical structure. Evidently, however, a series layer, if thin as is the case of the capped sputtered structures, will not be penal and higher permittivity silica-alumina sol-gel films may be used if the processing is easier than for pure silica.

It should be noted in all the above calculations that the assumption is made that the composite feature size is small compared to wavelength. Even for 10 GHz frequency components, the wavelength is of order 1 cm in a material

of relative permittivity 10 so this is likely to be valid for all cases of interest here.

#### 4.0 MACRO-DEFECT-FREE CEMENTS

##### 4.1 Introduction

This area of study is under the direction of Dr. D.M. Roy and encompasses the work of three graduate assistants, Paul Sliva who is studying calcium aluminate cement, Marianella Perez who is exploring the properties of Imperial Chemical Industries MDF cements and comparing these with commercial Type I, II and III cements, and Pamela Kistler who is making a study of the processing of ASTM Type II cements to obtain strengths comparable to the MDF materials.

Reasons for initiating studies in this area of chemically bonded ceramics for substrate applications are:

(i) In the chemical consolidation process of the cement curing, there is a change of phase to a hydrated form which is of lower density than the parent powder; thus it is in principle possible to obtain full mechanical integrity without shrinkage. Since for most ceramic tape systems, it is the reproducibility and control of shrinkage which limits wiring resolution and density, zero shrinkage could be most valuable.

(ii) The very low temperature "curing" of cement permits a very wide range of techniques for introducing a second phase, perhaps a fugitive phase which can be lost in subsequent processing to produce the controlled closed pore structures which are necessary for permittivity control.

In the hydrated consolidated cement, the exact character of the bound water is not well understood, and it is not clear how this hydrated phase will affect the high frequency dielectric loss behavior or how this property will be modified by the wide range of process variables in the preparation of the cement. An urgent priority in these initial studies was the characterization

of the dielectric loss for a range of cements under different process conditions.

For each of the classes of cements, it is necessary to go through:

- (1) characterization of the precursor cements.
- (2) investigation of the possible processing methods to produce macro-defect-free character, and their influence on the dielectric properties.
- (3) Determination of the effects of additives, particularly silica micro-balloons to reduce the observed permittivity levels.

To conserve space and avoid a too prolix report, detailed preparation and characterization will only be given for one cement type, the calcium aluminate cements and in the other cases only salient differences in processing and results will be covered.

## 4.2 Calcium Aluminate Cements

### 4.2.1 Characterization of the Precursor Cements

Two suppliers of cements, Lone Star LeFarge, Inc. and ALCOA, produce several grades of high alumina or calcium aluminate cement. There are eight calcium aluminate cements being utilized in this investigation. Initial characterization of these cements include: i) chemical composition, ii) phase composition, iii) density, iv) surface area, and v) particle size distribution.

4.2.1.1 Chemical Composition. Table 4.1 summarizes the chemical composition of the cements under consideration. The five Lone Star cements are classified as SECAR cement followed by a number depicting the weight percent  $\text{Al}_2\text{O}_3$  content. ALCOA cements are classified by application or use. All of the ALCOA cements possess similar chemistry. The SECAR cements are comprised predominantly of  $\text{Al}_2\text{O}_3$  and  $\text{CaO}$ , except for SECAR 60 which contains a



Table 4.1 Thermal analysis of Secar and Alcoa Calcium  
Aluminate Cements

	SECAR 80 FAST SET	SECAR 60	SECAR 71	SECAR 80	SECAR 80 MODIFIED	ALCOA GUNNING GRADE	ALCOA CASTING GRADE	ALCOA RECHLAR GRADE
SiO <sub>2</sub>	0.32%	23.02%	0.52%	0.31%	0.35	0.30%	0.30%	0.32%
Al <sub>2</sub> O <sub>3</sub>	80.2	59.1	71.2	79.8	80.4	80.3	80.6	80.6
TiO <sub>2</sub>	0.008	0.58	0.013	0.008	0.908	<0.05	<0.05	<0.05
Fe <sub>2</sub> O <sub>3</sub>	0.07	0.38	0.11	0.07	0.07	0.27	0.27	0.26
MgO	0.19	0.19	0.38	0.20	0.26	0.09	0.09	0.05
CaO	17.7	13.3	27.5	16.7	16.5	17.7	17.1	17.3
MnO	<0.002	<0.002	<0.002	<0.002	<0.002	0.060	0.062	0.064
SrO	0.01	0.01	0.01	0.01	0.01	0.005	0.005	0.005
Na <sub>2</sub> O	0.45	0.22	0.37	0.74	0.95	0.51	0.58	0.56
K <sub>2</sub> O	0.02	0.10	0.04	0.02	0.02	0.04	0.04	0.02
P <sub>2</sub> O <sub>5</sub>	0.02	0.05	0.02	0.13	0.01	0.11	0.12	0.10
SO <sub>3</sub>	0.02	0.05	0.05	0.02	0.03	0.05	0.05	0.05
CO <sub>2</sub>	(0.29)	(0.28)	(0.09)	(0.44)	(0.55)	0.06	0.07	0.06
LOI (900°)	0.80	3.60	0.36	1.55	1.54	0.77	0.93	0.80
TOTALS	99.81%	100.60%	100.57%	99.56%	100.15%	100.20%	100.15%	100.13%

comparatively large quantity of  $\text{SiO}_2$ . Loss on ignition (LOI) percents are up to 900°C and contain the  $\text{CO}_2$  losses.

4.2.1.2 Phase Composition. Phase analysis by powder x-ray diffraction indicates a similarity in the phase composition of all of the calcium aluminate cements. Table 4.2 summarizes the phase composition of each of the cements. CA and  $\text{CA}_2$  are the predominant phases with S, A,  $\text{C}_{12}\text{A}_{14}$  present in varying amounts depending on the subtle variations in chemistry between the cements. The presence of  $\text{SiO}_2$  in SECAR 60 is expected since SECAR 60 is the only cement with a high enough Si chemical content to form a detectable Si compound.

4.2.1.3 Density. Densities were obtained by pycnometry using a non-wetting liquid (kerosene) and measuring the volume displacement for a known weight of cement. Densities of the calcium aluminate cements are given in Table 4.3. All other densities in this report are geometric densities.

4.2.1.4 Surface Area. Surface areas were obtained using gas adsorption on a known quantity of sample and range from 5 to 20 square meters per gram.

4.2.1.5 Particle Size Distribution. Particle size distribution of the cements by x-ray beam attenuation resulted in very similar curves. A representative distribution curve, ALCOA casting grade, is shown in Figure 4.1. Typical mean particle size (50% cumulative mass percent) of the cement ranges from 2 to 10 micron.

#### 4.2.2 Processing Methods

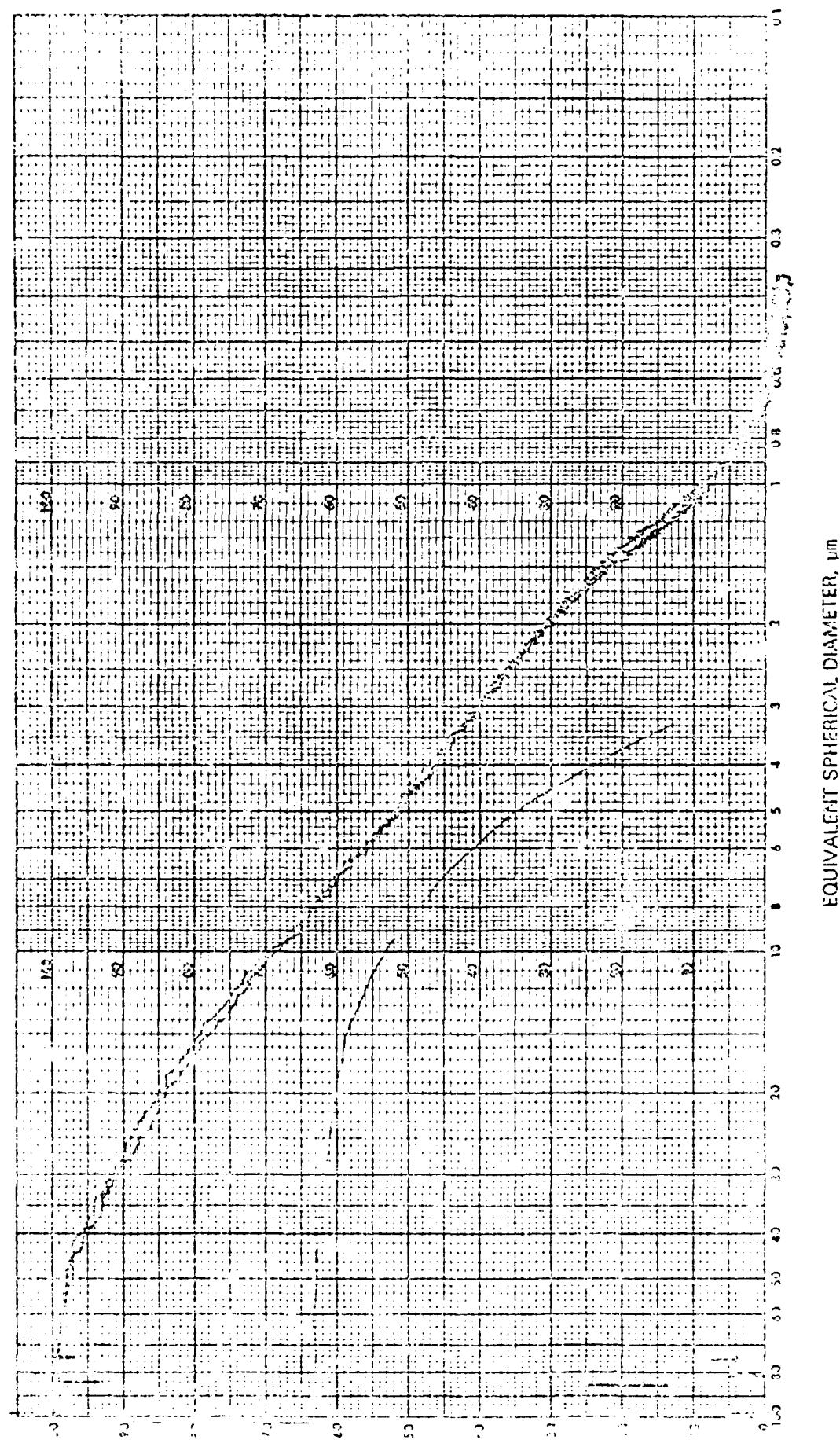
The major thrust of the fabrication studies of the cement pastes over this first contract year has been the use of high shear mixing to form the macro-defect-free (MDF) structure. The concept of MDF processing is basically

Table 4.2. Phases Present in Calcium Aluminate Cements.

Cement	Phase Composition*
SECAR 60	CA, CA <sub>2</sub> , S
SECAR 71	CA, CA <sub>2</sub>
SECAR 80	CA, CA <sub>2</sub> , A
SECAR 80 Modified	CA, CA <sub>2</sub> , A
SECAR 80 Fast Set	CA, CA <sub>2</sub> , A
ALCOA Regular Grade	Ca, CA <sub>2</sub> , A, C <sub>12</sub> A <sub>7</sub>
ALCOA Gunning Grade	CA, CA <sub>2</sub> , A, C <sub>12</sub> A <sub>7</sub>
ALCOA Casting Grade	CA, CA <sub>2</sub> , A, C <sub>12</sub> A <sub>7</sub>

Table 4.3. Density of Calcium Aluminate Cements\*.

Cement	Density (g/cc)
SECAR 60	2.95
SECAR 71	2.96
SECAR 80	3.12
SECAR 80 Modified	3.15
SECAR 80 Fast Set	3.18
ALCOA Regular Grade	3.22
ALCOA Gunning Grade	3.16
ALCOA Casting Grade	3.21



**Figure 4.1.** Particle Size Distribution of Alcoa Casting Grade Calcium Aluminate  
Decumulative (X-ray Sedigraph Technique).

to eliminate all but the finest pores in the cement in order to increase mechanical strength. An equally important consequence of MDF processing is the relative ease of fabrication to shape by uniaxial pressing, calendering extrusion or combinations of these techniques.

Following the ICI process pioneered by Birchall and co-workers, the very fine cement powder is mixed with a plasticizer (polyvinyl alcohol for these calcium aluminate cements, proprietary plasticizers in the silicate materials) high shear mixing in a commercial brabender mixer, followed by uniaxial pressing to form thin disks.

4.2.2.1 Shear Mixing: General Procedure. The shear mixing process involves the formation of a plastic cement dough by combining deionized water, calcium aluminate cement powder, and 80% hydrolized polyvinyl alcohol (PVA). A typical mix would consist of 11.11 gms of 10 wt% PVA solution, 50 gms of cement giving ratios of water/cement of 0.20 and (water + cement)/PVA of 0.018.

The dough is first mixed by hand until all free PVA solution is absorbed then it is homogenized and trapped air is removed by high shear mixing under vacuum in a CW Brabender preparation mill. The charge is typically 80 cc in a batch. The resulting dough is then weighed into 2 to 3 gm charges placed in a one inch steel die coated with a teflon mold release. Pressing into disks is accomplished by application of 4 to 30,000 psi pressure for 10-15 seconds, followed by a slow release. The pressure cycle is repeated three times to ensure the escape of any trapped air in the sample.

If the curing of the cement takes place in air at ambient temperature, the sample is removed from the die, otherwise for 80-85°C curing (above the softening point of PVA), the sample is maintained in the die under a nominal 200 psi pressure over the full curing cycle.

#### 4.2.3 Dielectric Response

Typical low frequency dielectric response for the secar cements is given in Figure 4.2(a) for the frequency range from 1 kHz to 1 MHz. In spite of the fact that these samples contain both unbound water and PVA, the permittivities are quite low. Dielectric loss in these untreated samples is typically of the form shown for the type 60 in Figure 4.2(b), decreasing to less than 3% at 1 MHz.

In the ALCOA cements, the response is similar for the air dried untreated samples, Fig. 4.3(a), with loss decreasing with increasing frequency, Fig. 4.3(b). Densities of the measured cement types are given in Table 4.4.

Experiments to address the effects of cold pressing to enhance densification of the cement paste show that for pressures up to 30,000 psi, at room temperature, there is no significant change in density (Table 4.5) and not surprisingly, no clear trend was evident in dielectric response.

Following ICI practice, curing of the cement at elevated temperature of order 80°C above the softening temperature of PVA was tried and gave much more dramatic change in dielectric response. For disks cured at 80°C even under nominal pressure of 100-200 psi, the density is increased by up to 20%. This rather small change of density, however, makes a major change in low frequency dielectric loss in all cement types, increasing loss levels at all frequencies by almost an order of magnitude.

It would appear that in these low temperature cured cements, the dominant transport of charge is in the residual water:PVA network, and that warm pressing to increase the coherence of this network thus greatly increases transport and associated low frequency loss.

It should be noted that the aluminate cements have not yet been subjected to the higher temperature post curing treatments discussed for the silicate

# DIELECTRIC CONSTANT OF CALCIUM ALUMINATE CEMENTS

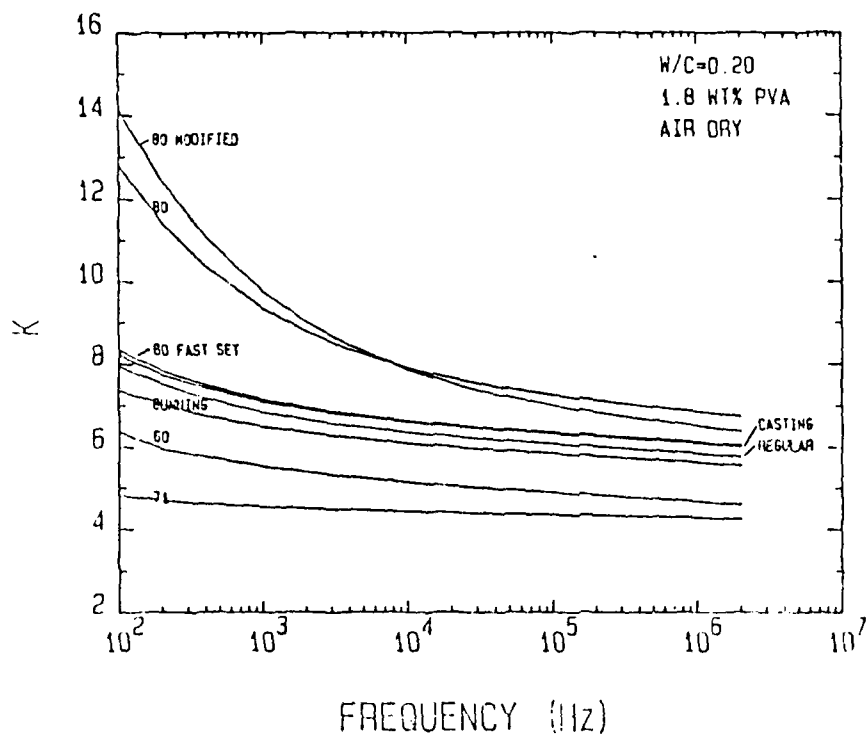


Figure 4.2(a). Dielectric Constant vs Frequency in Calcium Aluminate Cements.

60P-2018-AIR

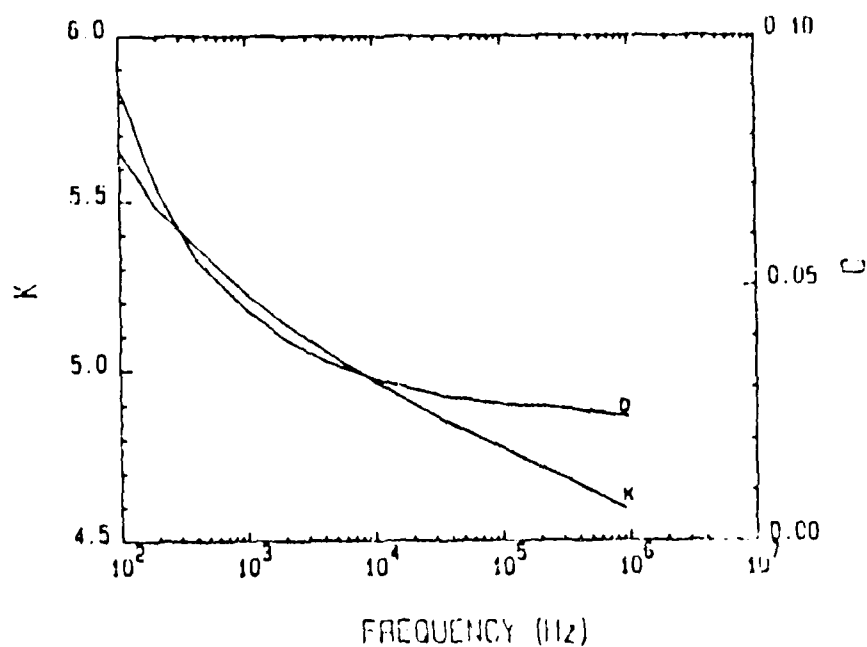


Figure 4.2(b). Dielectric Constant and Loss vs Frequency in Type 60 Calcium Aluminate Cement.



# DIELECTRIC CONSTANT OF ALCOA CEMENTS

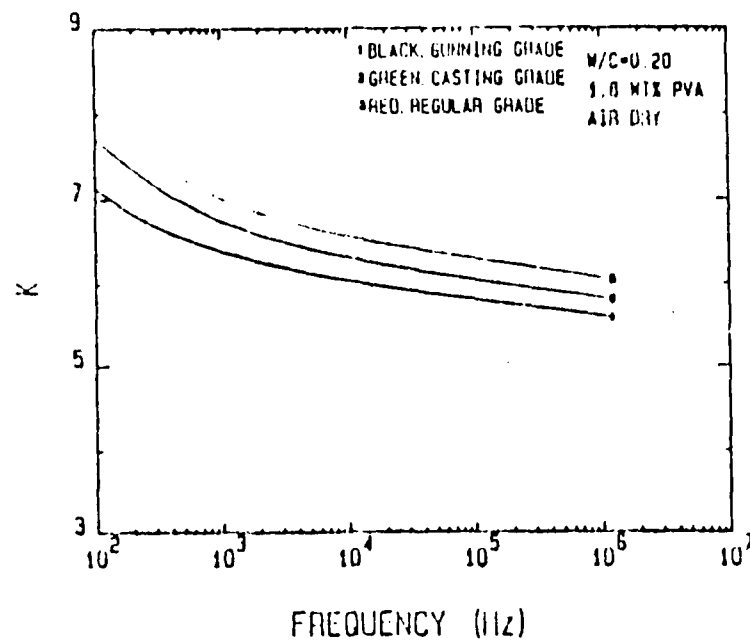


Figure 4.3(a). Dielectric Constant vs Frequency in ALCOA Cements.

## GNP-2018-AIR

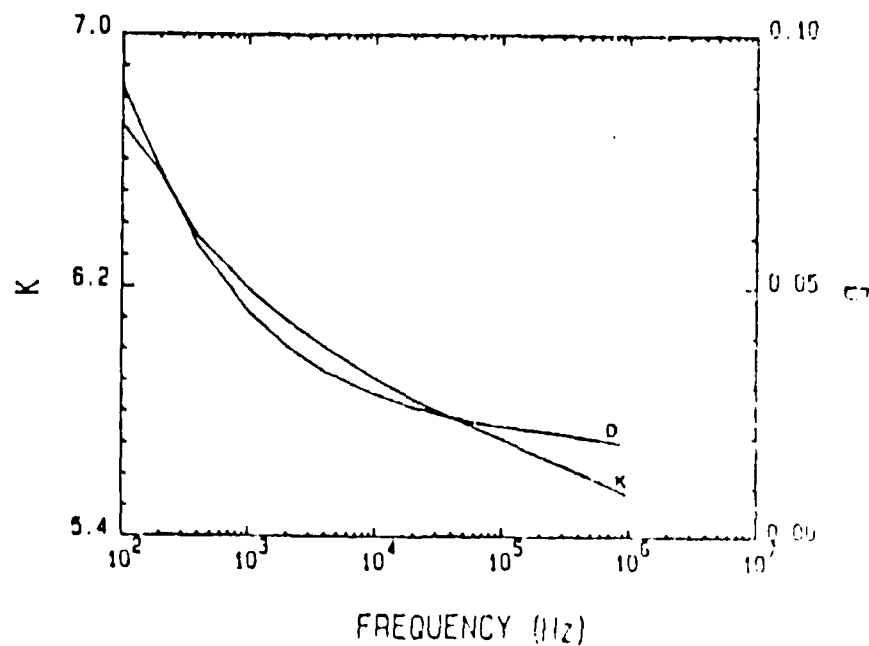


Figure 4.3(b). Typical Dielectric Constant and Loss vs Frequency in ALCOA Casting Grade Cement.

Table 4.4

Cement	Thickness	Density
Secar 60	2.67 mm	1.92 g/cc
Secar 71	2.67	1.88
Secar 80	2.61	1.89
Secar 80 Modified	2.59	2.04
Secar 80 Fast Set	2.46	2.29
ALCOA Regular Grade	2.34	2.21
ALCOA Casting Grade	2.41	2.18
ALCOA Gunning Grade	2.39	2.19

Table 4.5. Densities of Secar 71 and Secar 80 Discs Pressed at Various Fabrication Pressures.

Pressure	Secar 71	Secar 80 (No PVA)	Secar 80 (with PVA)
4000 psi	1.85 g/cc	2.00 g/cc	2.02 g/cc
6000	1.86	2.04	2.07
8000	1.89	2.12	2.22
10,000	1.91	2.13	2.23
12,000	1.95	2.11	2.30
14,000	1.97	2.15	2.22
16,000	2.00	--	2.12
18,000	1.95	2.35	2.12
20,000	2.00	2.23	2.00
30,000	--	2.37	--

cements, and it will be most interesting to observe the changes in loss spectra as free water is expelled from these differently prepared cements.

#### 4.2.4 Effects of Additives

The dielectric permittivities accessible with the aluminate cements, as with all other inorganic insulators, are too high for the Ga:As packaging requirements. To modify the cement host and make a lower permittivity composite, preliminary studies have been made of the effect of adding silica glass micro-balloons.

High strength hydrospace micro-balloon spheres are manufactured by Emerson and Cuming under the trade name Eccosphere FTD-202. The micro-spheres have an average diameter of 65  $\mu$  meter, a wall thickness of order 1-2  $\mu$  meter, a permittivity of 1.17 and a dissipation factor less than 0.0013 over the frequency range 1 MHz to 8.6 GHz.

To test out the influence on the dielectric response, a Secar 80 cement was chosen. The echospheres were added to the cement dough then the whole was homogenized in the Brabender mixer.

Permittivity as a function of frequency at room temperature for 0, 20, 30, 40, 50 and 60 vol% loadings are given in Fig. 4.4. Evidently, the permittivity at all frequencies is lowered and the maximum depression occurs at 30 vol% loading. Presumably at higher loadings the cement paste is unable to screen the spheres from breakage in the mixer.

From the mixing formula, the cement:echosphere composite should exhibit almost ideal Maxwell mixing. For the lowest frequency, the change observed is from

$$K = 15.5 \text{ to } K = 6.6 \text{ at } 30\% \text{ loading}$$

while at the highest frequency measured,

$$K = 6.7 \text{ to } K = 5.0 \text{ at } 30\% \text{ loading.}$$

# DIELECTRIC CONSTANT AS A FUNCTION OF MICROSPHERE LOADING

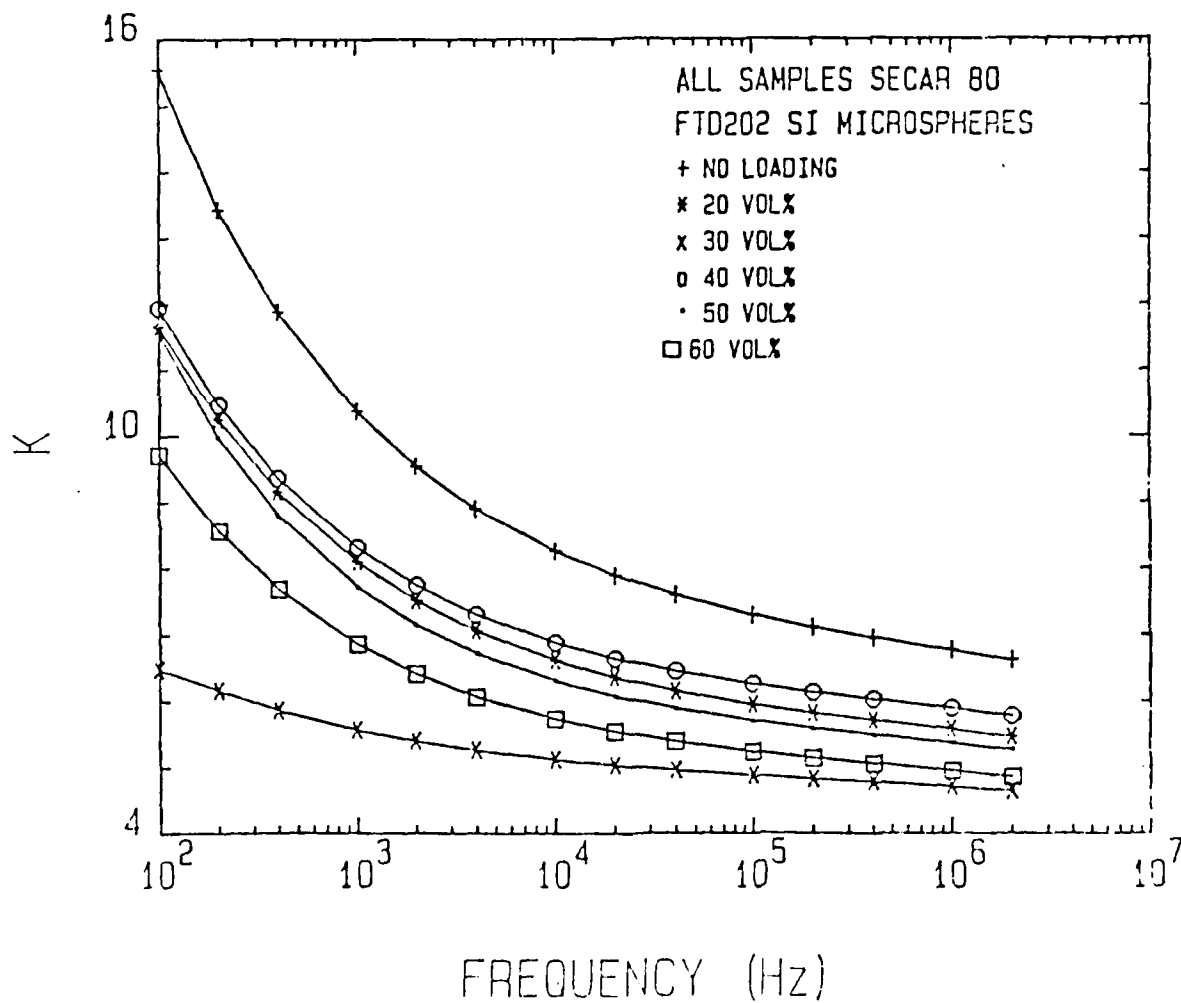


Figure 4.4. Dielectric Constant vs Frequency in Calcium Aluminate Cements with Various Volume Loading of Silica Micro-Balloons.

From the Maxwell formula, the values should be

$$K = 15.5 \text{ down to } K = 9.9 \text{ at } 30\% \text{ vol}$$

$$K = 6.7 \text{ down to } K = 4.2 \text{ at } 30\% \text{ vol}$$

Evidently, the higher K at low frequency in the pure cement system is a Maxwell:Wagner enhanced value and the echospheres are changing the character of the composite dielectric. At the higher frequency, the data should be reliable and the higher measured value would suggest that the processing is still breaking a significant fraction of the echospheres even at the 30% loading.

#### 4.2.5 Silicate Cements

Studies by P. Kistler and M. Perez, under the direction of Dr. D.M. Roy, have encompassed the portland cements of type 1, 2, and 3 and a micro-fine type z-62 cement.

In general, the processing steps are similar in the formulation of the cement except that proprietary plasticizers were used in place of polyvinyl alcohol, with a retarder often added to facilitate mixing.

Additional facets of work on the silicate cements have been:

- (a) More detailed examination of the shrinkage upon consolidation.

For a typical type II portland cement set under a humid atmosphere at 80°C then heat treated at 450°C to remove residual water and organics, the total shrinkage was only 2.8%, almost one order of magnitude smaller than in a conventional sinter-densified ceramic.

- (b) Heat treatments to improve low frequency dielectric properties.

In a type I cement after curing at low temperature as for the aluminate cements, samples were subjected to slow heating to 450°C, then maintained at that temperature for 1 hour. Subsequent weak field dielectric permittivity

measurements (Figs. 4.5 and 4.6) show very much reduced low frequency loss with room temperature values below 0.01 over the whole frequency range.

(c) Preliminary high frequency measurements on both normal and micro-fine cements which have been heat treated to 450°C confirm the absence of any absorption peak in the range 1.0 to 3.0 GHz where water losses would be expected to obtrude.

(d) Additional processing steps which have been studied to improve density and reduce open porosity have included:

- (1) Uniaxial cold pressing
- (2) Uniaxial warm pressing (80°C)
- (3) Isostatic hot pressing
- (4) Isostatic pressing of coated samples
- (5) Extrusion followed by HIP treatment
- (6) Microwave curing.

Steps (2) and (5) appear to be most effective to date, and more extensive suites of samples are now being made up for mechanical and electrical testing.

(3) experiments with silica micro-balloons again point up a problem of breakage in the mixing step, under the high shear condition of the Brabender mill - more benign techniques for inserting the second phase are now under study.

## 5.0 SOL-GEL PROCESSING

### 5.1 Introduction

The objective of these studies which are under the direction of Dr. R. Roy, and involve the work of two graduate students, W. Yarborough and U. Mohideen, are two fold.

(1) To explore the possibilities for using the sol-gel method to form films which are thick enough to support multilevel wiring but whose

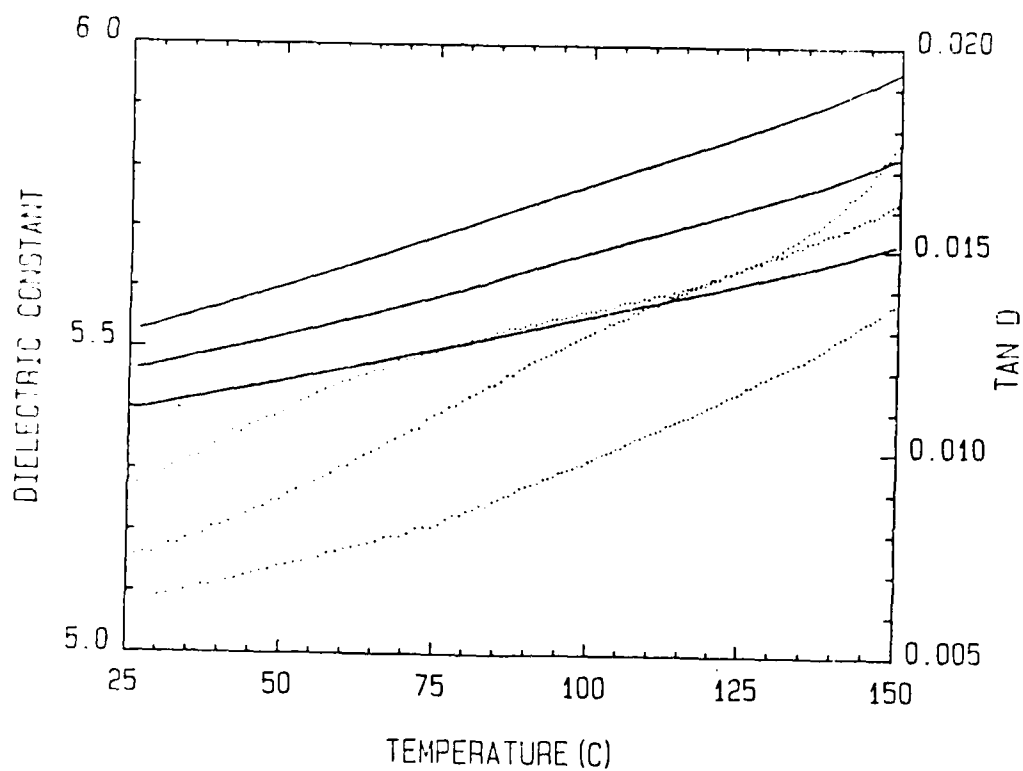


Figure 4.5. Type I Portland Cement After Heat Treatment to 450°C for 1 Hour.

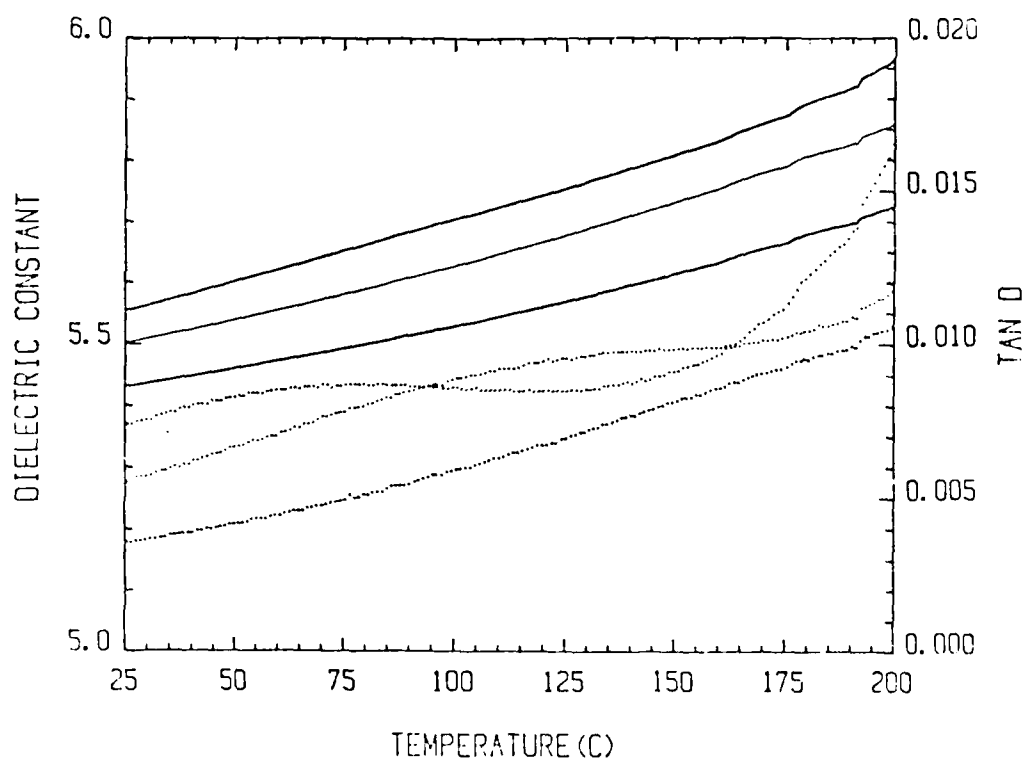


Figure 4.6. Type I Portland Cement Second Heat Treatment.



composition, density and microstructure can be controlled to give ultra-low permittivity and low loss.

(2) To develop much thinner coatings which can be processed to yield high density zero porosity silica or silicate glass and could be applied to "seal" porous structures developed by sputtering, etching, or other techniques.

Basically, Yarborough has been focusing primarily upon task (1), while Mohideen has been expending effort on task (2) though there is necessarily considerable overlap.

## 5.2 Thick Film Studies

### 5.2.1 Introduction

Materials have been prepared using colloidal  $\text{SiO}_2$  sols and dispersable boehmite having permittivities less than 6 and loss tangents less than about 2% at frequencies greater than 1 MHz. In addition, we have found that low density, very high  $\text{SiO}_2$  (>95 wt%) materials can be prepared using silica sols doped with aluminum oxalate solutions. For reasons which are not yet fully understood, doping with aluminum oxalate produces high gel volumes with reduced shrinkage on drying, and virtually no shrinkage or densification on calcination to temperatures of 900°C. Diphasic gels in the  $\text{Al}_2\text{O}_3/\text{SiO}_2$  systems of >50 wt%  $\text{SiO}_2$  do not appear to have as great a tendency towards cracking as do either of the end members. This offers the potential of preparing (with the proper processing) porous NCS materials, stable against devitrification to temperatures of 1200°C. Hence a large proportion of effort has been directed towards developing an understanding of this system and the various options for processing. A wide range of compositions and densities have been prepared with moderate progress in controlling the tendency of such materials to warp and/or crack on drying and firing. However, this remains a major problem.

Densities obtained range from less than  $1 \text{ gm/cm}^3$  to approximately  $2.3 \text{ gm/cm}^3$  (the density of fused  $\text{SiO}_2$ ). Strength remains a serious concern with fired xerogels of high interconnected porosity. Firing has been done in air using temperatures of  $1200^\circ\text{C}$  or less. Effort is continuing to obtain reasonable strength with retained porosity at firing temperatures of  $900^\circ\text{C}$  or less for compatibility with high conductivity metals (Cu or Ag)..

Preliminary work has been completed on the possibility of using diphasic organic/inorganic gels as a route to controlling gel formation and densification. Of particular interest is the possibility of using photopolymerizable resins or gels as a means of simultaneously controlling gel formation and forming vias and/or conductor paths.

#### 5.2.2 Experimental

$\text{SiO}_2$  Sols. Colloidal  $\text{SiO}_2$  have been used in all experiments to date. These include DuPont's Ludox formulations HS-30 and AS-40. These are 30 and 40 wt%  $\text{SiO}_2$  and are stabilized with NaOH and  $\text{NH}_4\text{OH}$ , respectively. It has been found that the presence of Na is highly detrimental, contributing to devitrification at temperatures as low as  $900^\circ\text{C}$ , particularly in the presence of small amounts of Al. Also it was noted in the course of XRD analyses of earlier preparations that color center development occurs on exposure to the x-ray source. It is suspected that the presence of Na contributed to this and could lead to degradation in dielectric properties on exposure to radiation of the finished substrate. In addition, some contribution to the permittivity is suspected (Maxwell-Wagner effect). Work with NaOH stabilized sols was abandoned in favor of  $\text{NH}_3$  stabilized sols. The AS-40 material also contains some Na contamination ( $\sim 0.08 \text{ wt\%}$  as  $\text{Na}_2\text{O}$ ) and this is still suspected to be a possible problem. Current experiments are being conducted by dispersing a pyrogenic silica (e.g., Cab-O-Sil MS-7SD,  $\sim 200 \text{ m}^2/\text{gm}$ ) of less than 2 ppm Na in

deionized water without stabilization. Unfortunately, this limits the solids content attainable with present equipment (about 20 wt%) and the shelf life of the sol (about 3 to 5 days). Also to be tested is a high  $\text{SiO}_2$  sol (>30 wt%), using this source of  $\text{SiO}_2$ , stabilized with  $\text{NH}_3$  or quaternary ammonium bases of high purity. Tetrethyl or tetramethylammonium hydroxide is preferred.

$\text{Al}_2\text{O}_3$  Sources. A dispersible microcrystalline boehmite (Disperal) has been used to prepare the  $\text{AlOOH}$  sols used. In addition, an aluminum oxalate has been prepared in the laboratory. The latter is prepared by the direct reaction of Al powder with oxalic acid in water at 90 to 95°C. To date, a suitable commercial source for the latter has not been found.

Diphasic Gel Preparation. Table 5.1 lists the results to date. Experiments have been conducted using four different preparative methods which should produce quite different levels of porosity with different types of microstructures. These are:

- (1) Gelling of colloidal silica with various additives to produce a porous, monophasic xerogel.
- (2) Ultrasonic dispersion of disperal directly in a  $\text{SiO}_2$  sol.
- (3) Preparation of a  $\text{AlOOH}$  sol from the disperal (using  $\text{HNO}_3$  for peptization) and subsequent addition of  $\text{SiO}_2$  sol while mixing at high speed.
- (4) Addition of a 0.1 M  $\text{Al}_2(\text{C}_2\text{O}_4)_3$  soln. to a silica sol.

#### 5.2.3 Diphasic Organic/Inorganic Gels

One of the major obstacles encountered in the attempt to use gels is that they are brittle and weak in the partially dried or green state. Although dense strong ceramics can be obtained on calcination, most gels fragment on drying and/or in the early stages of sintering. There are methods available

Table 5.1. Data Summary.

Expt. No.	Composition and Method	Firing Temp. and Time	Relative Permittivity	Loss Tangent	Frequency Range
36-1	Disperal and Ludox AS-40 w/Al oxalate 33.3% alumina Ultrasonified	1200°C/2hrs.	5.4-5.7	0.01-0.002	1 KHz-1 GHz
36-4	Disperal and Ludox AS-40 w/o Al oxalate 32.5% alumina Ultrasonified	1200°/2hrs.	5.2-5.9	0.03-0.01	1 MHz-1 GHz
38-3	Disperal and Ludox AS-40 w/Al oxalate 39.7% alumina Ultrasonified	1200°C/2hrs.	5.1-5.9	0.02-0.004	1 KHz-10 MHz
65-2	Cab-O-Sil L90 sol w/Al oxalate 1.37% alumina sol/solution	900°C/2hrs.	2.2-2.81	0.06-0.4	1 KHz-100 KHz
67-2	Cab-O-Sil MS-7SD	900°C/2hrs.	1.83-1.89	0.002-0.01	1 KHz-100 KHz
71-1	sol w/polyethylene-imine sol/solution		1.69-1.80	0.0016-0.01	

to avoid this problem (notably critical point drying). However, a suitable substrate technology must allow for the formation of vias and possibly other substructures. The current practice of punching holes in a green tape is not likely to be feasible with gels. It may be possible to overcome this by selective gelation using a fugitive network forming composition. Employing a suitable chemistry, one might picture a process such as that outlined in Figure 5.1. Alternatively, a low density silica xerogel may be saturated with resin, masked, exposed to form the desired pattern, unreacted material can then be washed away and vias etched with HF. (The cured resin protecting the substrate where left unmasked.)

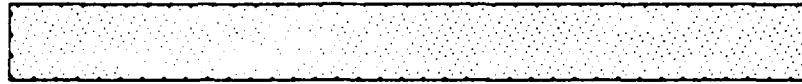
Preliminary work has been done using acrylamide as the primary monomer, crosslinking with either the ammonium salt of 2,2-Bis(acrylamido)acetic acid or N,n'-Methylenediacrylamide. Initiation has been with ammonium persulfate and tetramethylethylenediamine. Initial results indicate that oxygen inhibition and non-uniform gelation are likely to be the major barriers to a successful process. If feasibility can be demonstrated, intentions would be to use a compound such as AIBN, i.e. 2,2'-Azobis(2-methylpropionitrile), as a photoinitiator in combination with UV radiation. Nitrogen blanking may be necessary to overcome the oxygen inhibition.

#### 5.2.4 Vapor Deposited Diphasic Materials

Examination of the data in Table 1 shows that a low density silica xerogel, stable to at least 900 degrees C, can be prepared to give permittivities as low as 1.6-1.8. These materials are not likely to be useful as they are quite fragile with open, highly interconnected porosity and high surface area. It is potentially possible to reinforce these materials and seal their surfaces against the atmosphere by chemical vapor impregnation/deposition. It may even be feasible to do this in a single operation by

Figure 5.1. Outline of Proposed Process for Via Formation in Low Density Gels.

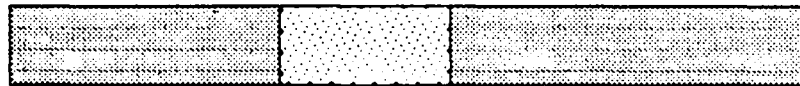
Multi-functional monomers are dissolved with suitable photoinitiators and accelerators in a sol and cast or coated onto a carrier web (e.g., Mylar).



Areas desired as vias are masked, and casting exposed to radiation of appropriate energy level for the initiator being used (typically UV or EB).



Those regions left unmasked are gelled by polymer gel formation, and the masked portions remain liquid:



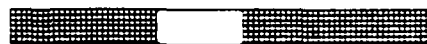
Unreacted material is readily washed away to leave via.



Polymer is burned away at relatively low temperatures, leaving low density xerogel



Body densified by high temperature firing



varying the substrate temperature and gas pressure. The type of microstructure envisioned is seen in Figure 5.2. The proposed second phase would be silicon nitride or a silicon oxynitride.

#### 5.2.5 Current and Future Work

##### Immediately:

- \* Obtain density estimates and microstructural characterization for xerogels with permittivity data.
- \* Attempt measurement of hardness and  $K_{10}$  values, including if possible an estimate of environmental effects.
- \* Begin empirical correlations of density, permittivity, fracture toughness, microstructure and composition.
- \* Prepare series of triphasic gels of composition:  $Al_2O_3/SiO_2$ /cross-linked polyacrylamide to determine if cracking/warping can be eliminated.

##### Longer Term:

- \* Explore effect of monofunctional/difunctional monomer ratio on gelation uniformity using low  $Na_2O$ , pyrogenic  $SiO_2$  sols and peroxide initiation.
- \* Compare behavior of peroxide initiated gelation with that obtained using a photoinitiator and UV source.
- \* Explore possible use of CVD/CVI for reinforcement of low density  $SiO_2$  xerogel.

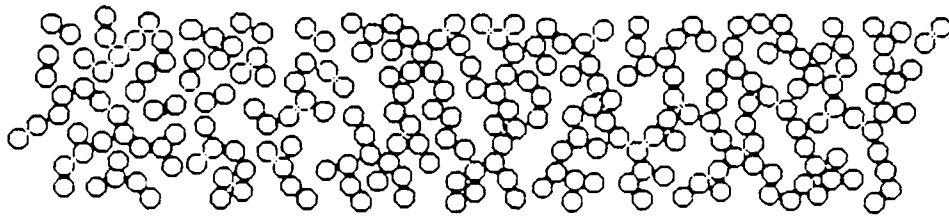
### 5.3 Thin Film Coatings

#### 5.3.1 Introduction

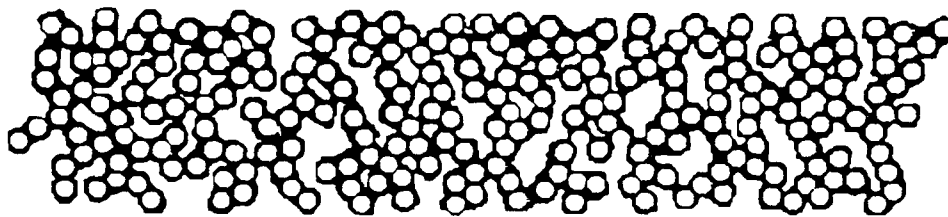
The primary focus of this work as discussed above was to develop the technique to make thin (1  $\mu m$  or less) films of  $SiO_2$  for capping etched structures made by sputtering or by other techniques. With the experience

Figure 5.2. Schematic Illustrating Use of CVI/CVD to Reinforce and Seal Low Density Silica Gel Microstructure.

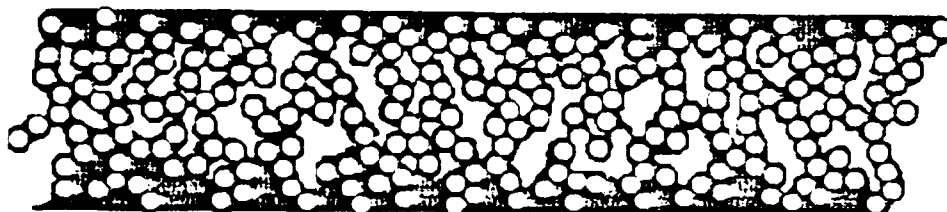
Schematic view of silica gel structure.



Gel structure after chemical vapor impregnation (CVI) with a reinforcing second phase.



Surfaces closed by chemical vapor deposition (CVD) of same phase (or a different phase in a separate processing step)





gained in developing and handling thin coatings, it was then hoped to be able to extend work to thicker coatings in the range up to 25  $\mu$  meter which would themselves be interesting as insulating support structures.

### 5.3.2 Experimental

(A) Sol-gel coatings of sputtered thin films were carried out successfully. For this purpose, sputtered porous GE films were used. These films were coated with organic precursor sols of compositions as given by Sakka, et al.<sup>(1)</sup>. Various methods of application of the coating such as dip coating, spray coating, and spin coating were considered. Of these, as is obvious, dip coating gave the most uniform film. The precursor sols were made of tetraethyl orthosilicate, ethyl alcohol, water and HCl or HNO<sub>3</sub>. These coatings are usually on the order of tenths of microns. Though a little cracking is still present on firing on these sputtered films, one can say with sufficient confidence from the vast experience with making SiO<sub>2</sub> thin films, that with slight variations of composition the cracks can be easily eliminated. At present, sol-gel coatings on porous sputtered SiO<sub>2</sub> films are being produced.

(B) A wide range of techniques has been explored to facilitate the development of thicker coatings, either by repeated thin coating or by single step thicker coating.

The experimental system in all cases is an SiO<sub>2</sub> or SiO<sub>2</sub>:Al<sub>2</sub>O<sub>3</sub> coating on a smooth silicon wafer surface.

Spray, dip and spin coating techniques have been explored, using the compositions suggested by Sakka, et al.<sup>(1)</sup>, Yoldas<sup>(2)</sup> and Nogami, et al.<sup>(3)</sup>. In every case, however, extensive cracking was observed on heat treatment when the coatings exceeded 0.5  $\mu$  in thickness.

The problem appears to arise from the very large capillary stresses from the high surface tension of water and the very small pore diameters (20-100A) in the gel.

Approaches being tried to improve properties include:

- (1) Increasing pore size by adding larger silica colloid particles.
- (2) Adding soluble phases to reduce the surface tension.
- (3) Changing the composition of the gel to reinforce the network.
- (4) Reducing the solvent content before coating by vacuum evaporation.
- (5) Adding a very fine fibrous phase to reinforce the gel network.

So far the best success has been accomplished by combining (1) and (3) replacing the usual tetraethyl orthosilicate with a trimethyl vinyl silane and dimethyl phenyl silane, using silica colloids from Nalco Corp. and adding aluminum dihydrogen phosphate to strengthen the gel during drying.

In this way smooth, well adhering crack-free films 1.5 microns thick have been produced which can be fired at 700°C without cracking.

## 6.0 LEACHED DIPHASIC GLASS STRUCTURES

### 6.1 Introduction

Work on the diphasic glass systems has been at a rather lower level. It is under the supervision of Dr. R.E. Newnham and involves the work of one graduate student, J. Yamamoto.

The focus has been to take commercially available glasses from Schott and from Corning and to measure dielectric properties both in as received and for leached porous structures.

### 6.2 Schott Glasses

The composition of the Schott glass is in the  $K_2O:B_2O_3:SiO_2$  family and the heat treatment used has resulted in a macro-porous structure. Scanning

electron micrographs (Fig. 6.1) show that the pore size is approximately 50  $\mu\text{m}$  and that the surface is correspondingly very rough.

For initial measurements, gold electrodes were sputter coated onto the major faces. Probe tests show that even on this very rough surface, the gold makes good contact, but penetration makes the final dimension difficult to define.

Measured dielectric permittivity is in the range 2.1 to 2.2 with dielectric loss less than .007 over the temperature range 20 to 125°C and the frequency range 100 kHz to 4 MHz.

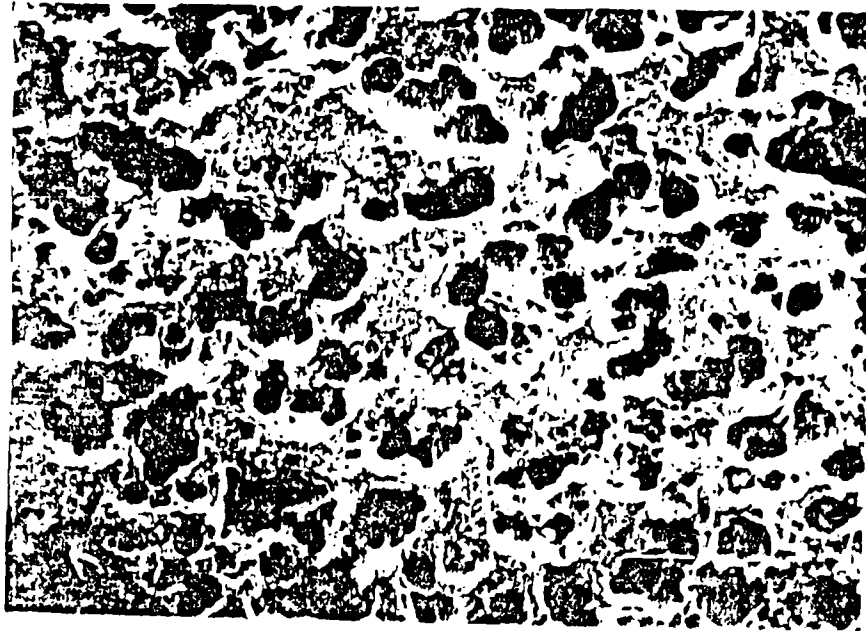
A second Schott sample, which had been heat treated to yield a smaller pore size gave permittivities in the range 1.8 to 2.0 and loss tangent less than .007 at 4 MHz.

Perhaps the major drawback to the Schott glass is its very coarse microstructure which leads to very rough surfaces that would certainly have to be capped to take normal metallization.

### 6.3 Corning Vycor Glass

The most promising porous glass medium to date is the porous Vycor manufactured by Corning. The pore structure in this material is on a much finer scale so that electroding by sputtering or evaporation is not a problem.

Measurements of permittivity and loss tangent over the range from 10 kHz to 4 MHz at temperatures from 25°C to 125°C show excellent low permittivity and loss (Fig. 6.2). To lower permittivity a little further, a post leaching with 10% HF was tried using leaching times of 2, 5 and 7 minutes. After leaching, samples were soaked in boiling dilute HCl to eliminate any impurities.



100µm

Figure 6.1. Scanning Electron Micrograph  
of Schott Porous Glass.

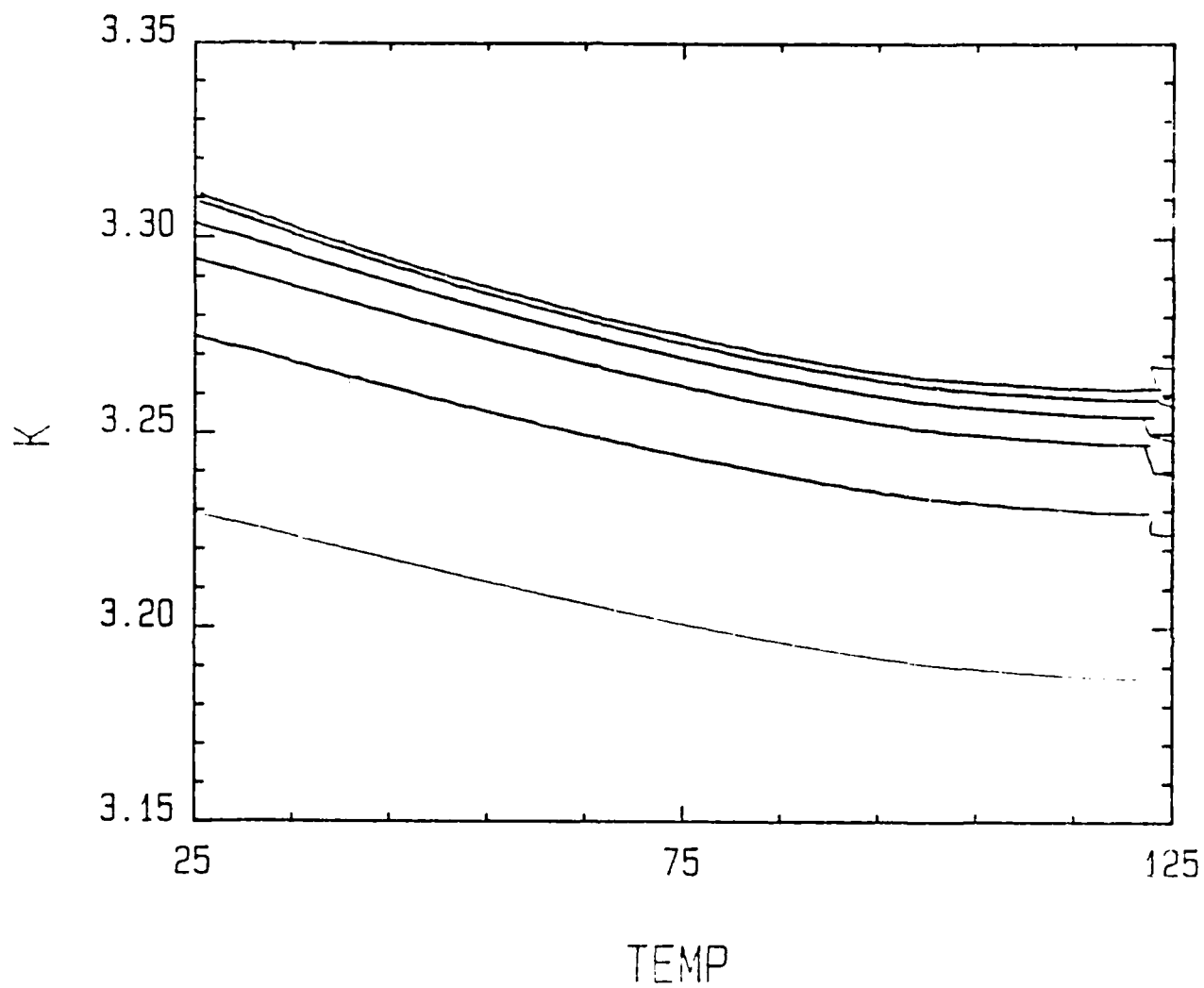


Figure 6.2. Dielectric Constant vs Frequency in a Corning Porous Vycor Glass at Frequencies from 10 kHz to 4 MHz.

Measurements at 1 MHz for the edge corrected permittivity are shown in Figure 6.3. It would not be expected to find enhanced permittivity or loss in these glasses at microwave frequencies and to confirm this, measurements were made using the resonant post technique. The values obtained were

$$K = 2.9 \pm .1$$

$$\tan \delta = .0045 \pm .0003$$

at 2.5 GHz, in good agreement with the lower frequency values.

All measurements on the Vycor were made after water:acetone wash, ultrasonic cleaning and heat treatment to 600°C in flowing O<sub>2</sub> gas.

#### 6.4 Future Studies

In the Vycor, leaching experiments will be extended to explore the range of accessible properties.

Microwave measurements will be extended to broaden the frequency range and to provide cross correlation between different techniques.

Surface treatments will be developed to render the etched surface impermeable.

In the Schott glasses, some studies will be attempted to cap the rough surface with a sol-gel coating and to improve the dielectric measurement. In parallel studies, we will also explore techniques for bonding silica micro-balloons to form a compact by using Al(H<sub>2</sub>PO<sub>4</sub>) as has been demonstrated by Verweij, et al.<sup>(4)</sup>.

### 7.0 SPUTTER DEPOSITED COATINGS

#### 7.1 Introduction

In this proposed approach, the objective is to make use of the highly anisotropic etching which occurs in sputtered films so as to generate a low

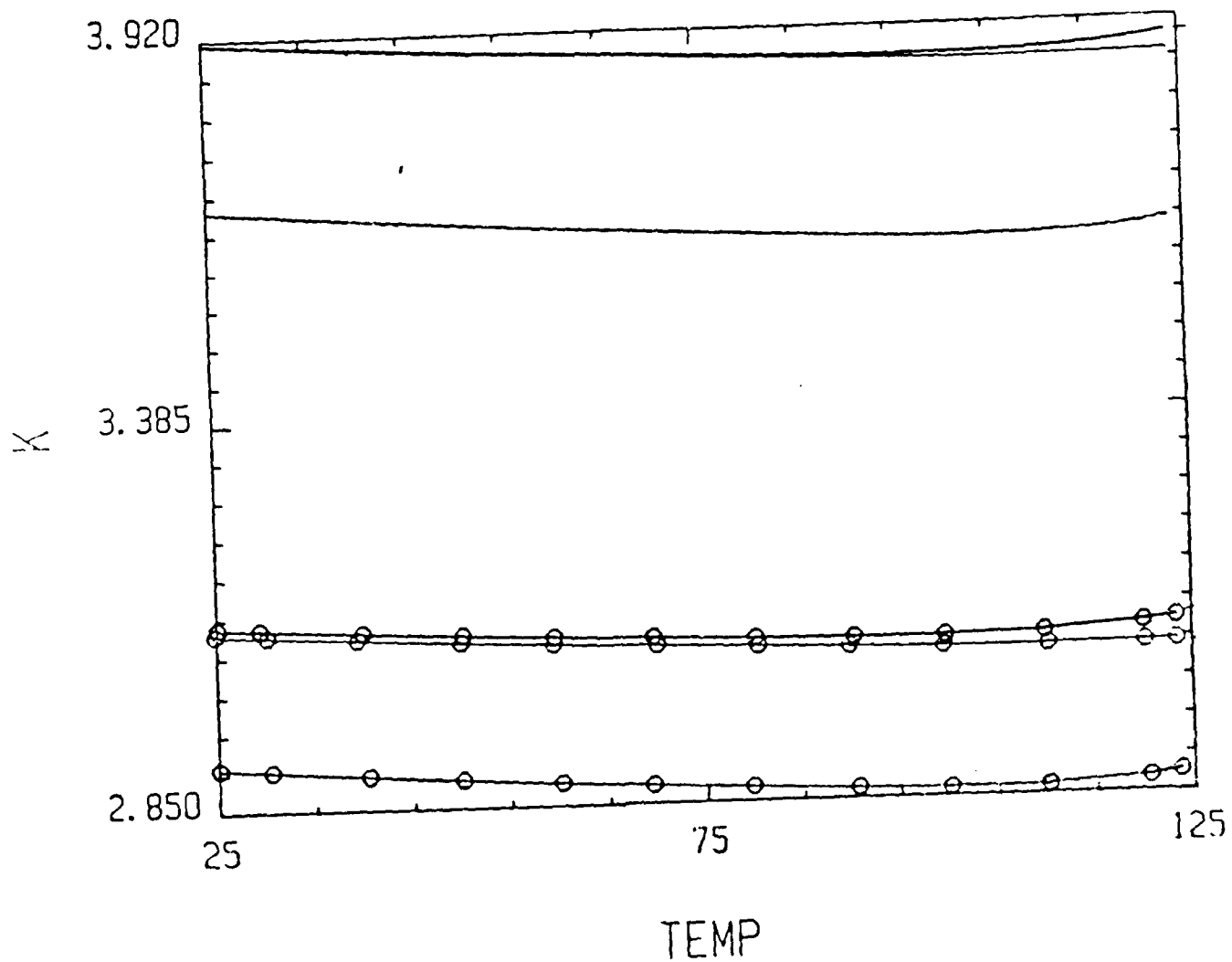


Figure 6.3. Edge Corrected Values of Permittivity for a Porous Vycor Glass Measured at 1 MHz. Data for 3 Typical Samples.

density structure of insulating pillars (Fig. 7.1) which could be capped by a thin sol-gel derived film to provide a support for the strip line traces.

By appropriate masking, the etched pore structure can be confined to the required low permittivity regions, retaining the strength and thermal conductivity of the bulk material in other areas.

For the original studies, several alternative processing routes were proposed (Fig. 7.2). In fact, over the first year we have demonstrated that while excellent insulator films can be produced directly in  $\text{SiO}_2$ , for our own simple AC sputtering systems the deposition rates are very slow and time consuming. Thus we have chosen to concentrate on the route using sputtered silicon which can be etched to the appropriate structure, then oxidized to  $\text{SiO}_2$ .

## 7.2 Deposition of Amorphous Silicon

Since the surface of sputtered films closely mimics the substrate upon which the film is deposited, it is essential to have smooth planar substrates. For these initial studies, polished single crystal silicon wafers were used. To permit reliable measurements of the dielectric properties of the sputtered films, a platinum film was deposited on the silicon  $\sim 200\text{\AA}$  thick to provide a high conductivity surface.

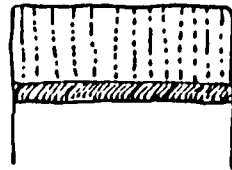
In order to control the fractal properties of the sputtered film it is necessary to define the sputtering parameters. Earlier studies had shown that by sputtering under high argon pressure, the mean free path of the sputtered species is kept short. This lowers the bombardment of the film, lowering the mobility of the species on the surface and thus enhancing self shadowing and consequent density fluctuations, so that strongly columnar films are formed.

For optimum coverage and suitable etchability, the following sputtering parameters were finally chosen.

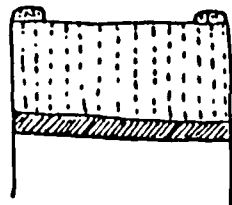




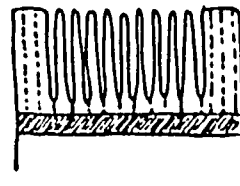
Metallized Substrate



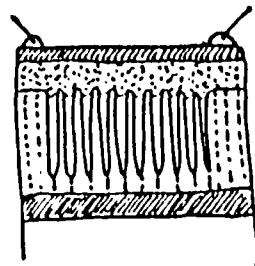
1. Deposit Coating  
(a-Si or a-SiO<sub>2</sub>)



2. Mask
  - 2a. Pattern mask (photoresist)
  - 2b. seed coating mask (~100Å of metal)



3. Etch (chemical, plasma, ion beam)
  - 3a. Remove mask
  - 3b. Oxidize (Thermal, plasma, ion beam)



4. Cap (Silica Gel Coating)
  - 4a. anneal (or other post-deposition treatment)
  - 4b. metallize → solder

Figure 7.1. Proposed Steps Involved in the Fabrication of the Sputtered Low Permittivity Film Structures.

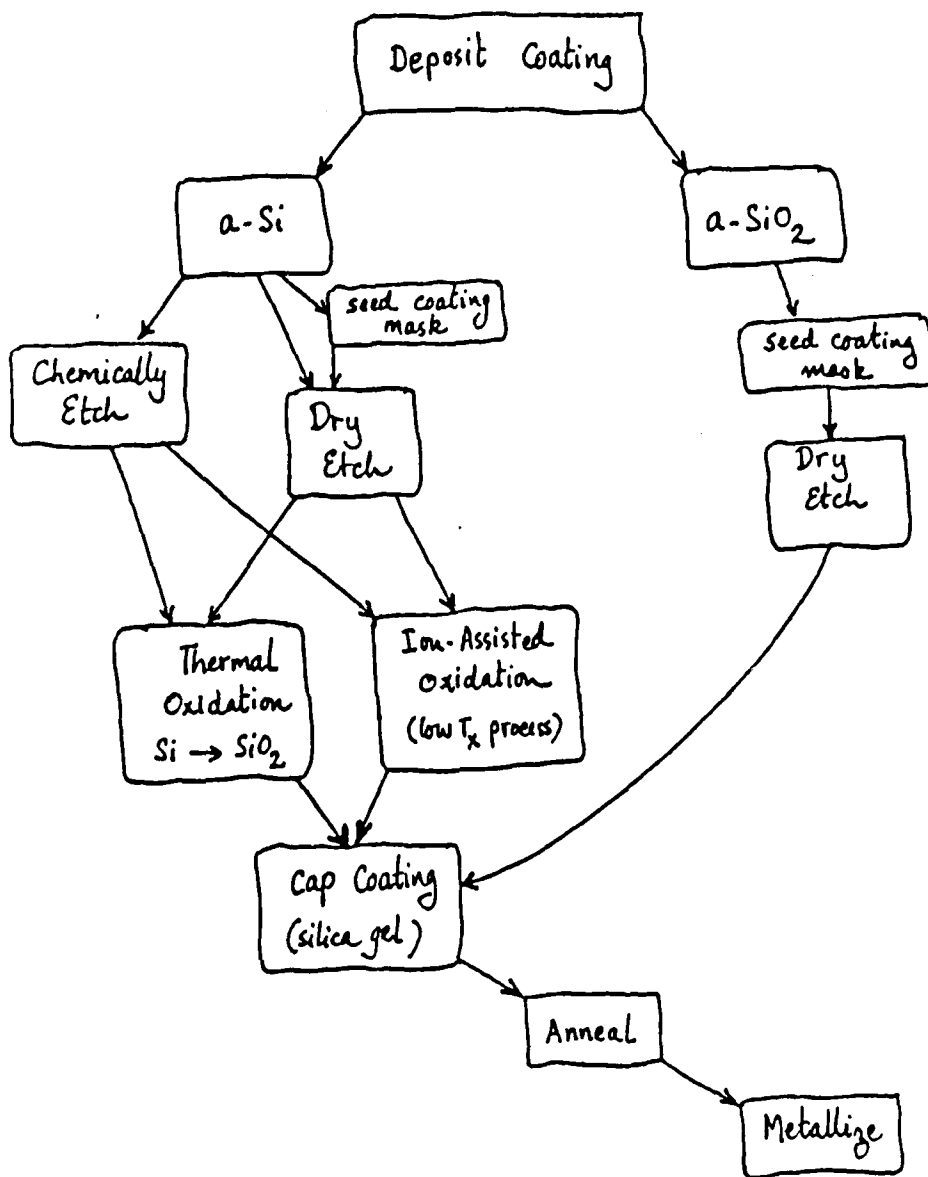
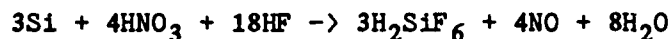


Figure 7.2. Alternative Processing Routes for Sputtered Etched Low Permittivity Film Structures.

Argon Pressure 30 mtorr  
RF Voltage 600  
Forward Power 70 watts  
Reflected Power 0 watts  
Plate Current 0.18 amps  
Presputtering Time 10 minutes  
Substrate:Target Distance 2.6 cm  
Total Sputtering Time 20 hours  
Total Film Thickness 25  $\mu$  meters  
Sputtering Rate ~ 210A/minute.

### 7.3 Anisotropic Etching

The chemical etchant used was a mixture of 90% HF to 10% HNO<sub>3</sub> by volume. Dissolution of the silicon is by an oxidation-reduction process, where HNO<sub>3</sub> is the oxidant and HF dissolves the oxidized silicon according to the reaction



With the low concentration of HNO<sub>3</sub>, oxidation is the rate limiting step. Low density regions are very rapidly oxidized, exposing the higher density columns.

The "stacked match" structure evident in Figure 7.3 is a good example of the highly anisotropic etching which can be achieved by proper application of the chemical method.

The planar upper surface of the film is also evident from the higher magnification scanning electron micrograph of a section of film, tilted at 30° with respect to the detector.

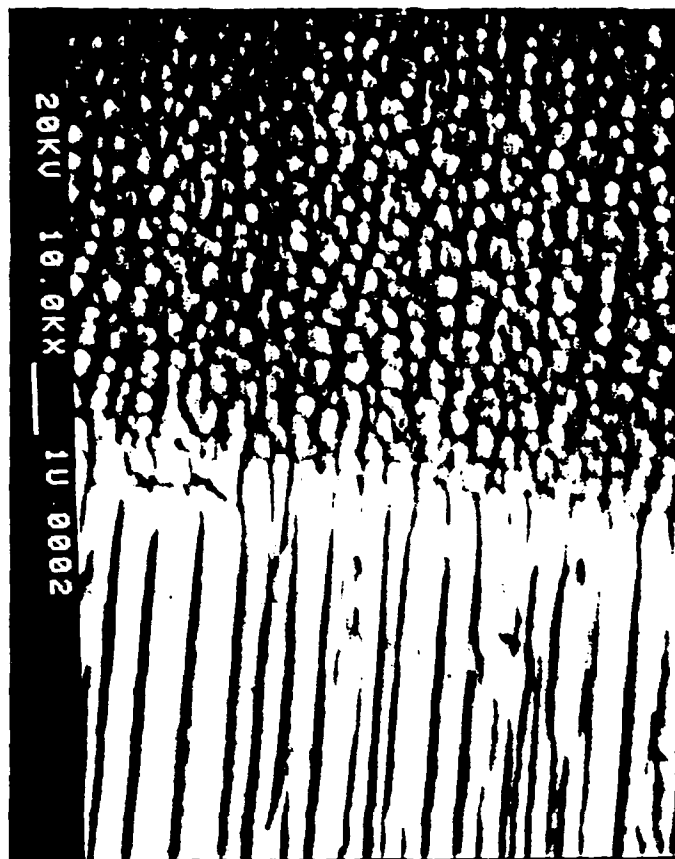


Figure 7.3(a). Structure of an Etched Sputtered Film of Silicon. (Note White 1 Micron Bar.)

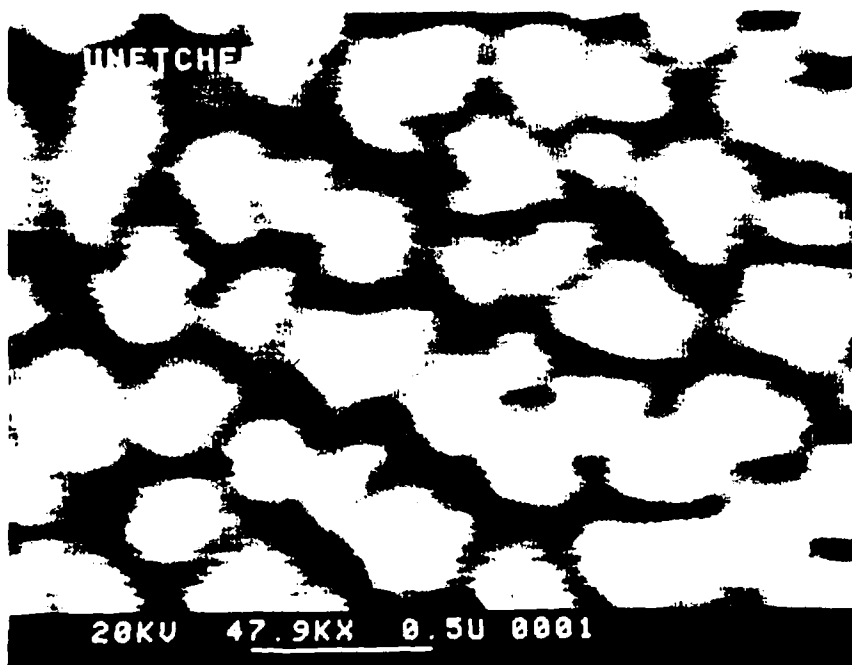


Figure 7.3(b). Higher Magnification SEM of Etched Silicon Surface (Tilt Angle 30°).

#### 7.4 Thermal Oxidation

Initial studies using flowing oxygen in an open tube furnace at 1000°C proved unsuccessful in affecting a complete conversion to  $\text{SiO}_2$ . Current experiments are now going forward in a closed system where the  $\text{O}_2$  pressure can be continuously monitored.

#### 7.5 Sol-Gel Coating

As discussed under the section on sol-gel processing model studies on columnar silicon and germanium surface have shown that by simple dip coating, it is possible to deposit a thin ( $0.1 \mu$ ) silica coating which does not penetrate down the columns. The coated films could be fired at 350°C for 12 hours to remove organic components to yield crack free (Fig. 7.4).

#### 7.6 Summary

25  $\mu$  thick sputter deposited films of silicon have been produced and a chemical etching technique developed which reveals the very strong columnar anisotropy.

Oxidation of the silicon columns could not be carried out in the simple open system used initially, and a closed system has now been constructed.

Preliminary capping studies have shown that a thin  $\text{SiO}_2$  capping film can be placed over the columnar structure by dip coating in a suitable gel, and that with a proper choice of viscosity, the gel does not penetrate the columnar system.

### 8.0 EVOLUTIONARY STUDIES

#### 8.1 Introduction

The role of Interamics in the joint PSU/Interamics program for the first year was to lower the permittivity (K) of alumina ceramic material by the

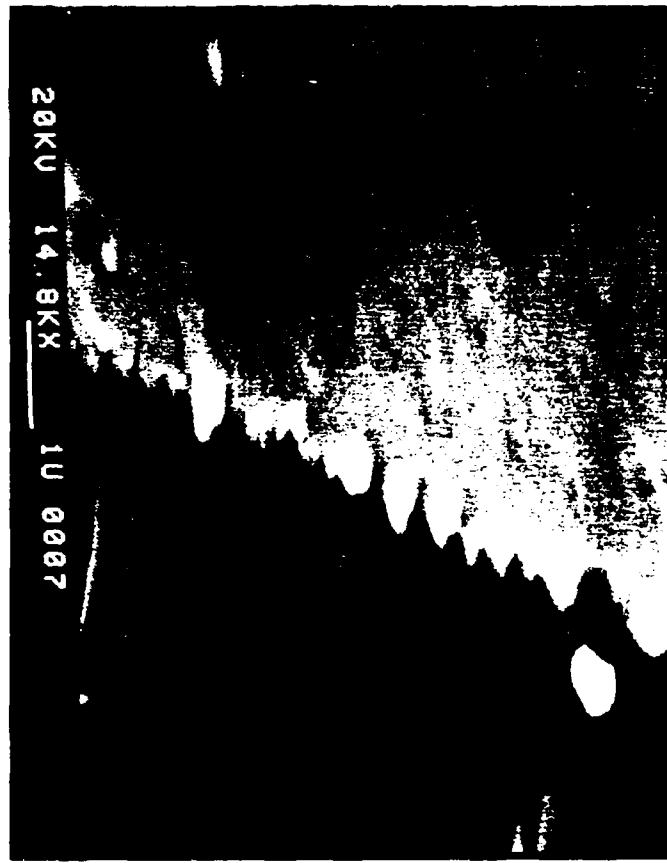


Figure 7.4. Sol-Gel Capping of a Model Etched Germanium Film.  
(Note White  $1\ \mu$  Scale Bar).

development of glass bonded ceramics (composites) for the packaging of GaAs integrated circuits and to develop a metal or metal system(s) that would result in higher electrical conductivity and finer line definition of the metallized patterns.

## 8.2 Approach to the Problem

In the evolutionary approach to the development of the low K ceramic composite, Interamics followed a proposed basic outline starting with the selection of raw materials that would be formulated into a ceramic body, adapted to the present tape casting process and finally metallized with low temperature metals used in the thick film industry. The initial investigation was to cover two ceramic/glass systems, alumina/glass and beryllia/glass. Since the beryllia system would require special health and safety equipment, the alumina/glass was selected for the immediate investigation.

For this investigation, a fine grained alumina and a lead-borosilicate glass, similar to that of the NEC composition, were selected for the study. A search for the ceramic raw materials and qualified vendors was conducted with a prime concern for chemical, physical, and electrical properties of the materials and the future availability and pricing. It was intended that the materials must be commercially available in substantial quantities for manufacturing purposes. The same would be required of the metallizing materials selected later in the program.

After considerable study, ALCOA A16 was selected for the alumina due to its similarity in particle size as reported by NEC.

Ferro Corporation, O'Hommel Company, Mobay Corporation (PEMCO), and General Color and Chemical (GCC) were contacted for technical data concerning lead borosilicate (LBS) and other frit materials having melting points in the temperature range of 760 to 950°C. Ferro Corporation did not respond at that

time. The O'Hommel materials were too high in sodium content which would be detrimental to the electrical properties of the ceramic. PEMCO has intentions of dropping the leaded frit materials in the near future. Samples were obtained, however, from both PEMCO and General Color and Chemical (GCC) having the following compositions and melting temperatures.

	<u>GCC GF-8</u>	<u>PEMCO (Pb 545P)</u>
PbO	44.5	61
B <sub>2</sub> O <sub>3</sub>	21.5	--
SiO <sub>2</sub>	34.0	36
Al <sub>2</sub> O <sub>3</sub>	--	3
M.P. (°C)	760	780

### 8.3 Preliminary Studies

The GCC frit (GF-8) was selected for the glass to be used in the initial investigation since it was the only true PBS material available.

The A-16 Al<sub>2</sub>O<sub>3</sub> and GF-8 were blended "as received" in small batches in the ratios by weight of 50/50, 55/45, and 60/40, respectively. The above blends were then mixed in a water solution of polyvinyl alcohol (binder) and oxyethylene/propylene (plasticizer). After drying this suspension at 100°C, the resulting cake was reduced to powder by mortar and pestle and screened through a 60 mesh (250 µm) sieve. Discs of each composition were pressed at 20,000 psi. Each disc had a surface area of one square inch and a thickness of approximately 1/8 inch. Samples of each composition were fired at 800, 850, 900, and 950°C with a 30 minute soak in an air atmosphere.

After firing, the diameter of each disc was measured and firing shrinkage was calculated. Dry, saturated, and suspended weights were made, and fired densities were calculated. The results of fired density and shrinkage are



shown in Figures 8.1 and 8.2. Visual observations were made after each firing noting color, surface texture, and glass adherence to the setters.

The measurements indicated that the 50/50 and 55/45 compositions were within a desirable firing range for forming packages, while the 60/40 composition appeared to be too refractory even at 950°C. The 50/50 composition reached peak density at 850-875°C, while the 55/45 reached it peak above 900°C. Above 900°C the 50/50 composition fused to the setter, indicating an extreme lowering of viscosity of the glassy phase.

Samples of each composition were broken purposely, exposing many bubbles in the interior which resulted in densities of 3.0 and 3.1 for compositions 55/45 and 50/50, respectively. The theoretical values for these compositions, calculated by the additive theory, was approximately 3.5 g/cc. This is evidence of improper firing and possibly poor dispersion of the frit material.

Since the above materials were used in their "as received" condition, the optimum results were not obtained. Particle size reduction by milling would increase the dispersion of the glass frit material and accelerate reaction and possibly lower the firing temperatures. A Fisher Sub-Sieve Sizer was ordered to measure the particle sizes of the incoming materials and results of all milling experiments. Additionally, the newly purchased microprocessor controlled furnace would result in improved firing capabilities and quality.

At the time when the milling studies were to commence, a sample of another frit material, a calcium borosilicate (CBS) frit (designated GF-125) was acquired from General Color and Chemical for this study. Samples of LBS and CBS were prepared by milling each for 1, 2, and 4 hours to attain various degrees of particle reduction. Unfortunately, the particle size measuring equipment had not arrived to measure this difference, therefore, only the one hour milled samples were studied.

A16/GF8 BODY

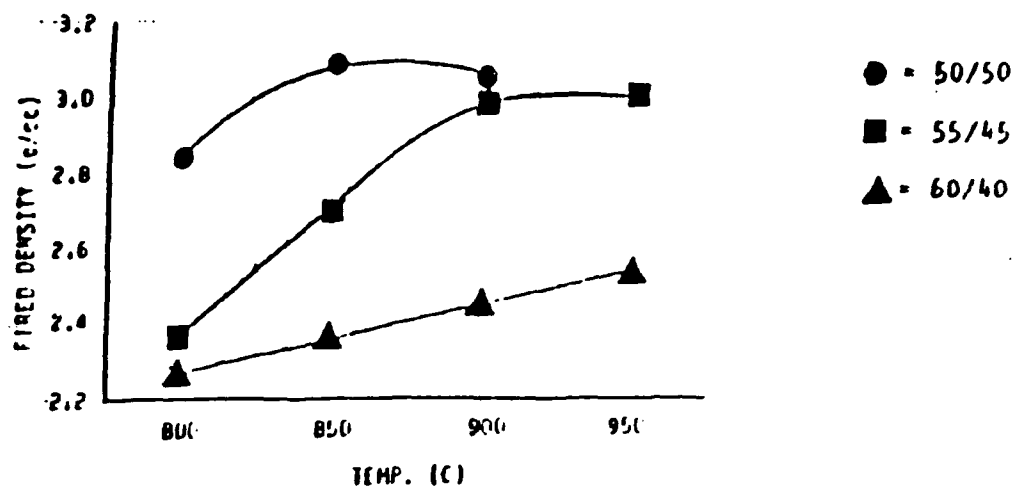


Figure 8.1. Fired Density vs. Temperature.

A16/GFB BODY

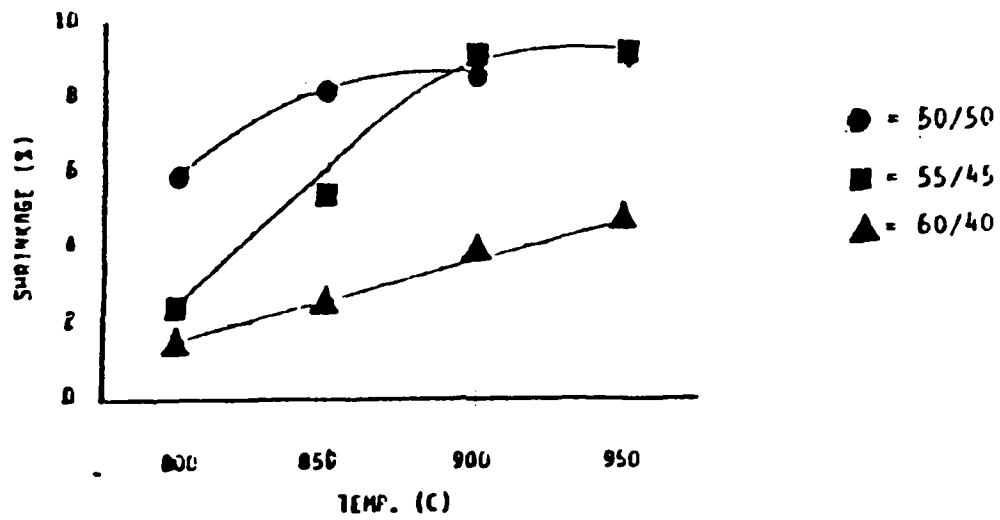
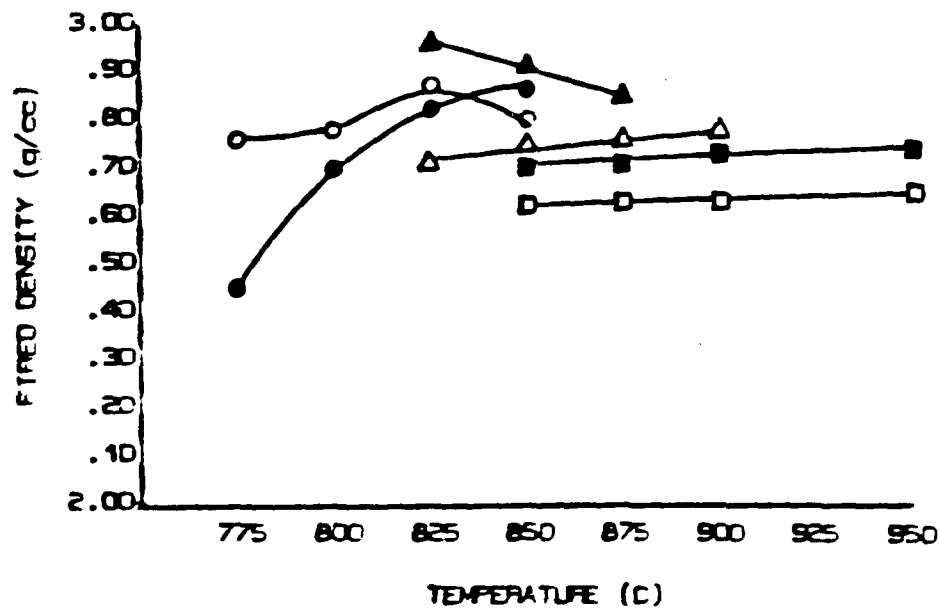
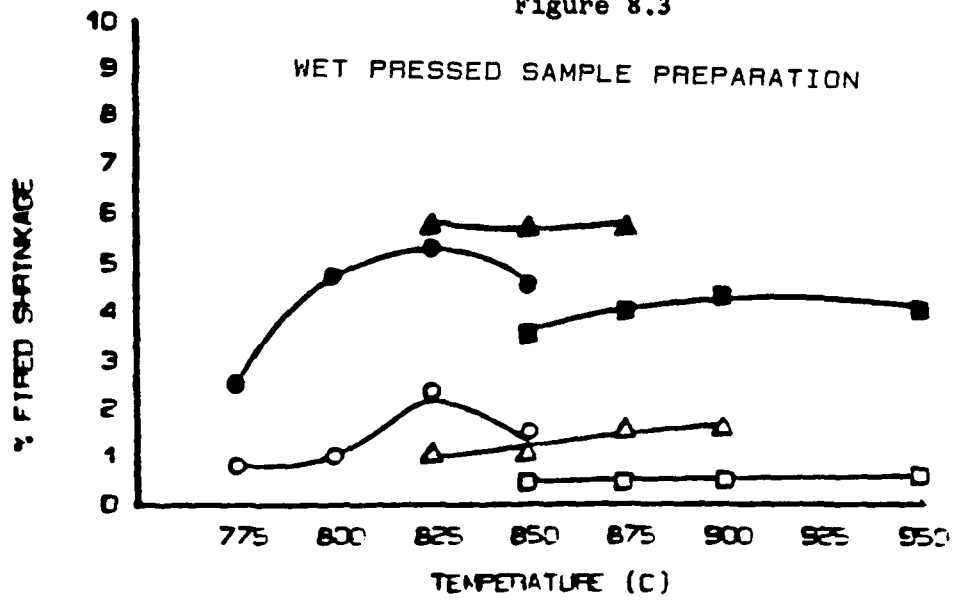


Figure 8.2. Shrinkage vs. Temperature.

Compositions with 60/40, 55/45, and 50/50 alumina/glass ratios were batched with both LBS, CBS, and A16 S.G. alumina. The materials were formed as aqueous suspensions containing a PVA binder, then force dried, granulated, and dry pressed at 20 Kpsi pressure. Due to migration of the binder during drying, many large irregular voids were detected internally after firing. Samples were then made as binder free, ethanol based slurries which were semi-wet pressed into discs after an appropriate drying period. The resultant samples were of sufficient quality to conduct firing studies and gather physical property data, despite the fact that small isolated air bubbles were present. The fired results of the study displaying shrinkage and density are shown in Figure 8.3.

Since densification and shrinkage appeared to stabilize in a desirable temperature range (850-900°C), the 55/45 composition was selected for further studies for both glasses in the conversion to ceramic tape. Many rheological problems were encountered during this conversion due to the differences in particle sizes and specific gravities of the materials. The initial study was directed to the development of a solvent/surfactant systems that would prevent gelling and high thixotropy of the slip. A workable system of polyvinyl butyral, ethanol/methyl iso-butyl ketone solvent, and refined Menhaden oil surfactant was derived. The frits were introduced into the slip in both the unmilled (as received) and milled (1 hour) states to note any rheological differences. Gelling of the slip and cracking problems in the tape were encountered, but with time, this was brought under control. Delamination occurred prior to and during firing, but a sufficient quantity of samples was made to complete the firing studies. The following results were obtained:

Figure 8.3



○—○	50/50	ALUMINA/LBS
●—●	50/50	ALUMINA/OBS
△—△	55/45	ALUMINA/LBS
▲—▲	55/45	ALUMINA/OBS
□—□	60/40	ALUMINA/LBS
■—■	60/40	ALUMINA/OBS

1. The use of milled frit is favored over unmilled material because it lowers the slip viscosity and improves the flow characteristics of the slip. The surface texture of the tape is also noticeably improved.
2. The fired densities of the tape bodies are lower than those of the pressed bodies. This is due in part to the difference in binder content and compaction mechanisms involved which may effect the level of internal voids. It appears that the chemistry of the frit material could also be responsible for the number and size of voids. The LBS body exhibits a coarser structure and larger, more irregular voids than the CBS composition. Therefore, it can be concluded that the low LBS density is due to its high level of voids. The cause is presently unknown.
3. It was interesting to note that the LBS containing samples matured at a higher temperature than the CBS samples. Since the melting points of the LBS and CBS materials are 760° and 954°C, respectively, the converse was expected. This suggests the possibility of reaction with the alumina, although this is unproven at this time.
4. The K of the LBS and CBS composites measured at Raychem were 5.3 and 7.4 respectively. NEC reported a K of 7.5 for an LBS composite of an identical ratio. It appears that the amounts of voids in the LBS body has diluted the K of the body.

#### 8.4 Particle-Size Reduction Studies

Earlier compositional studies indicated a significant difference between the one hour and four hour milled frits. The magnitude of this difference was unknown. Because particle size was found to have a great effect on rheology, a Fisher Sub-Sieve Sizer (SSS) was purchased to measure the particle size of

the materials used in the program. Although the unit lacks sophistication, it was proven to be a reliable and reproducible method for measuring equivalent spherical diameters. The particle size of all materials were measured in the "as received" condition to establish baseline data.

To further investigate the effects of particle size changes on slip rheology, a particle size reduction study of GCC frits by wet milling in ethanol was conducted. Ethanol was chosen to minimize any possible hydration of the borate glasses. Samples of the slurry were drawn at predetermined intervals, dried, and measured for particle size.

The results of this study would aid in obtaining specific particle sizes on demand, and establishing reproducibility in the system. The results were expressed graphically in Figure 8.4. Numerous rheological problems are encountered in systems using extremely fine powders. Twenty-four hour milled frit was selected because of its resultant particle size. It was believed that this materials would minimize rheological problems, and allow the formation of materials within a reasonable time frame for further testing.

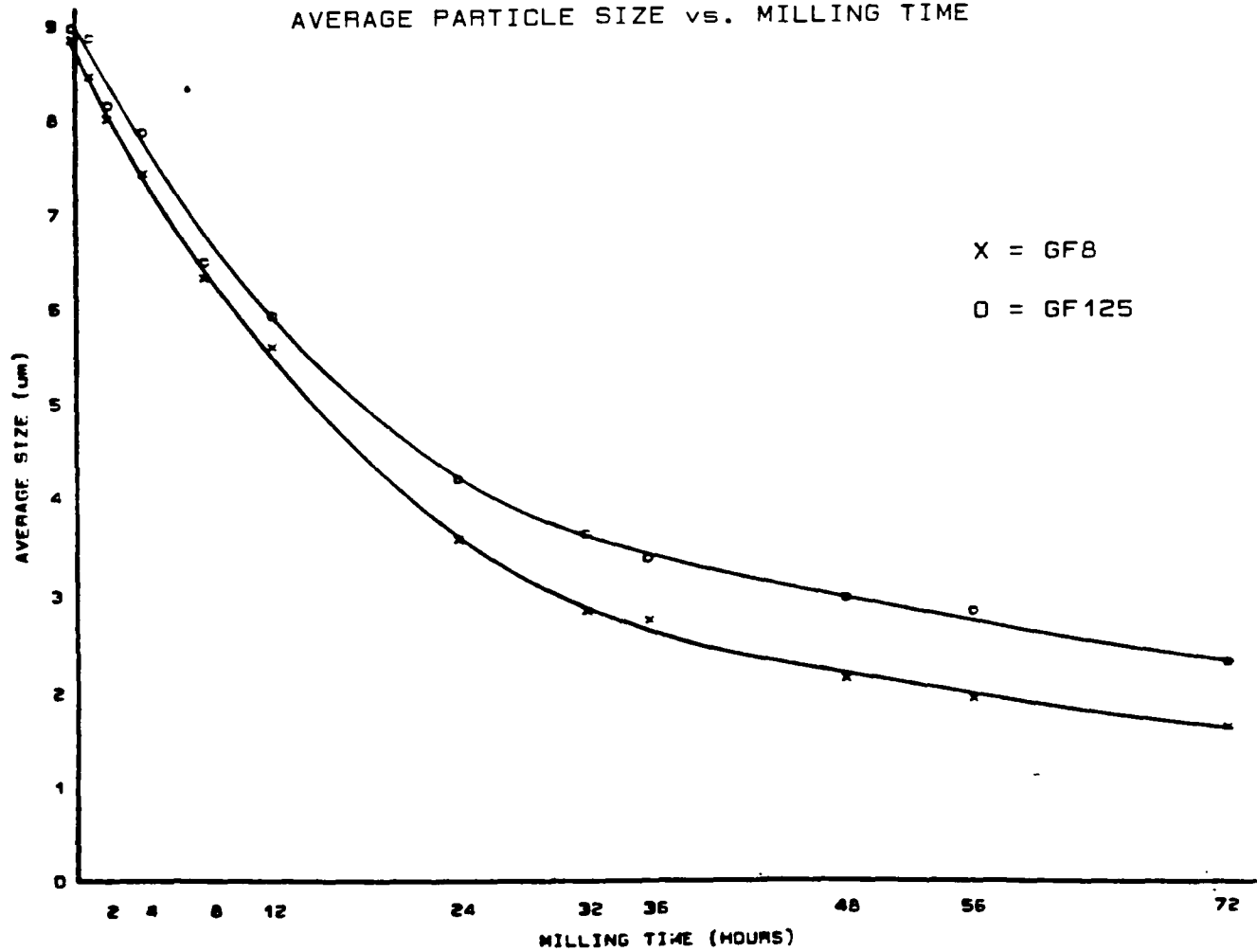
Using the 55/45 (alumina/frit) composition and organic vehicle system formulated earlier, the effort was focused on the development of two workable tapes. An acceptable tape should exhibit the following properties: 1) no cracking, 2) smooth surfaces to facilitate screening of conductor patterns, 3) easily stripped from the casting surface, 4) ability to be punched and handled repeatably, and 5) easily laminated. To attain these desirable tape characteristics, the slip from which it is made must have the following properties: 1) good flow characteristics, 2) quick leveling, 3) readily desirable, and 4) the ability to dry without cracking.

A considerably higher number of rheological problems was encountered with the 24 hours materials as when compared to the one hour materials utilized in the third quarter. The major problems were high viscosity, which resulted in

Figure 8.4

FRIT MILLING STUDY

AVERAGE PARTICLE SIZE vs. MILLING TIME





deairing problems and a thixotropic nature, and cracking during drying. Extensive modifications and variations of slip test batchings yielded successful formulas, resulting in acceptable tape. The rheology problems were resolved by altering the ratio of the vehicle constituents. It is believed that the rheology problems for this system have been solved and they are not due to inconsistent materials preparation. It should be noted that the 24 hour materials used for batching do not correlate exactly with the curves generated for the milling study, as shown below in Table 8.1. However, the batch to batch control of particle size is excellent (See Table 8.2). The lower particle size measurement of the milling study material may be attributed to overmilling due to a reduction in charge, caused by frequency slurry sampling.

Table 8.1. Particle Size Milling Study Vs. Batching.

	LBS	CBS
24 hour milling study	3.7	4.5
24 hour batch material	4.7	5.0

Another important condition in the control of the rheological behavior is an aging process. Aging while rolling at low RPM significantly reduced slip viscosity, and yielded crack free tape.

#### 8.5 Firing Studies

Cards 4.5" x 4.5" were blanked from the cast sheets, and laminated at 250°F/990 psi. One inch by one inch firing test specimens were punched from the five layer laminates.

Table 8.2

PARTICLE SIZE OF FRITS  
USED IN TEST BATCHINGS \*

LEAD FRIT:	BATCH NUMBER	AVERAGE SIZE ( $\mu\text{m}$ )
	1	4.4
	2	4.7
	3	4.7
	4	4.7
CALCIUM FRIT:	1	5.0
	2	5.6
	3	5.0
	4	5.0
	5	5.1
	6	5.0
	7	5.1

\* AS MEASURED BY FISHER SUB-SIEVE SIZER

The new firing profile (Fig. 8.5) was implemented which allowed for longer intermediate soak periods at the temperature ranges where: 1) the organic binder system volatilizes and 2) hydrated borate phases decompose to form  $B_2O_3$ . It is believed that the evolution of gases during these two temperature ranges was the cause for large amounts of internal porosity. Optimum firing temperatures were determined to be 830°C/10 minutes (CBS) and 940°C/10 minutes (LBS). Additional work on the design of furnace profiles is slated for next quarter, pending results of TGA and DTA analysis of samples which were presented to Dr. L.E. Cross at a meeting on 7/12/85.

Cross sectional analysis of both the CBS and LBS bodies fired with the new profile verified a significant reduction in internal void size, which now average 12.5  $\mu m$  in diameter. Reduction in void size and distribution may also be attributed to the milling of the initial materials and the resultant improved packing. The combination of improved firing methods and particle size reduction is therefore directly responsible for the following:

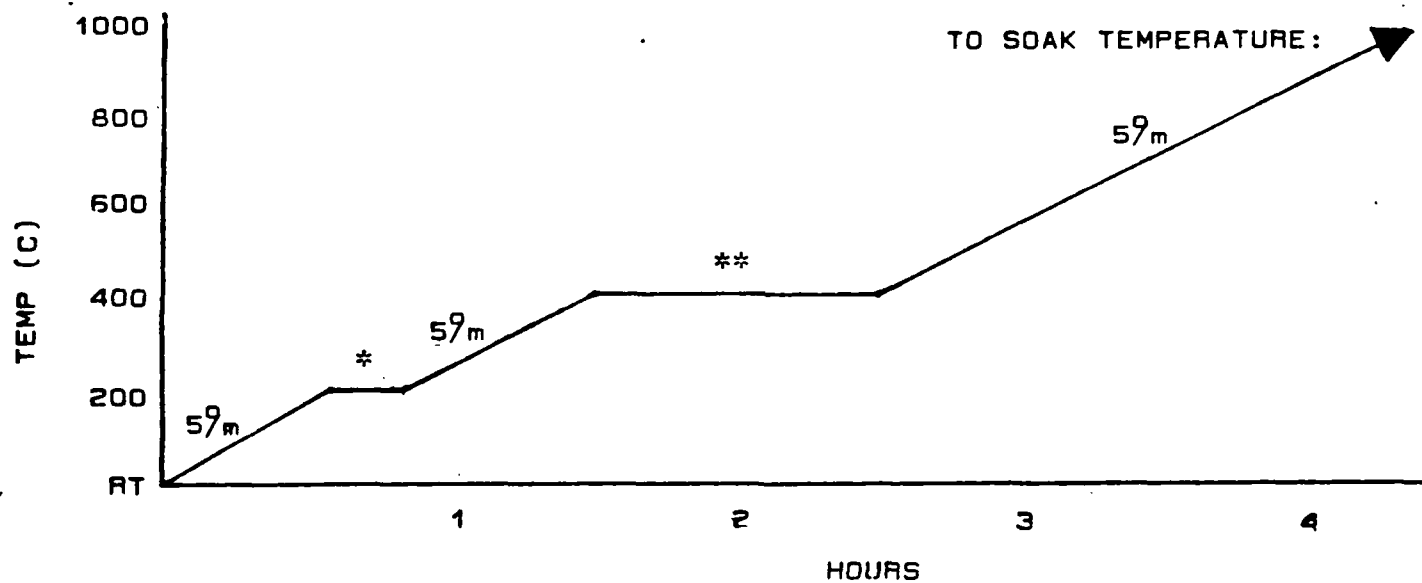
1. The reduction of size of internal porosity.
2. The reduction in quantity of internal porosity.
3. Increased fired density.
4. A vast improvement in cosmetic appearance.

Samples were sent to Raychem on 7/22/85 for dielectric constant measurement. Expectations are that the current bodies will exhibit higher dielectric constants than the previously measured samples. It is possible that the earlier measurements were lower than 7.5 due to a large amount of internal voids and possible undetected delaminations.

#### 8.6 Metallization Studies

Investigation of thick film metallizing materials was initiated during the fourth quarter. Information was obtained from DuPont, ESL, and EMCA

Figure 8.5  
FIRING PROFILE FOR  
TEST BODIES



\* BORON CHEMISTRY REACTION TEMPERATURE

\*\* ORGANIC VOLATILIZATION TEMPERATURE

concerning their conductor materials. Other vendors remain to be contacted. Samples of various silver pastes were obtained from Ceronics for use in the early stages of the metallizing program.

#### Summary

1. Commercially available raw materials were found to supply alumina and two glasses. Vendor reliability for the future has been established.
2. Through formulation and firing studies, a range of workable compositions was derived.
3. The effect of particle size on rheology of the tape systems was studied. Two workable tape systems were formulated.
4. Lamination and firing procedures were developed for the tape systems, permitting the formation of samples for dielectric constant, shrinkage, porosity, and density measurement. These resultant bodies will be utilized as a test vehicle for the remainder of the evolutionary portion of the program (i.e., metallizing, prototype package fabrication, etc.).
5. The investigation of thick film metallization materials was initiated. Samples, artwork, and a screen were obtained for early study. Information on other thick film materials was received from several sources.
6. A total of 2275.5 hours were expended on efforts during the first year of the program. A breakdown of the total can be found on Table 8.3 to account for the hours of the involved personnel.

#### Projected Studies

1. Metallizing materials will be tested during the coming quarter to observe the following:
  - a. The reaction with the ceramic composite.

Table 8.3

TOTAL HOURS AT INTERAMICS  
DEVOTED TO THE PSU PROGRAM  
DURING THE FIRST YEAR (1984-1985)

NAME	HOURS
PRADEEP GANDHI	225.0
JACK RUBIN	110.0
WARREN GYURK	555.0
ROB LUCERNONI	690.5
DAVE BRYAN	<u>695.0</u>
TOTAL	2275.5

- b. The requirement of frit within the metallizing paste to promote a bond to the ceramic.
  - c. The resultant bond strength.
  - d. The electrical conductivity
  - e. The effect of atmosphere on all of the above conditions.
  - f. Other materials will be investigated, such as gold, silver, palladium, silver-palladium, platinum and copper.
- 2. Reduction of the frit materials to the NEC range will be attempted. A solution to the rheological problems will be sought, and finalized formulae will be derived.
  - 3. Firing schedules will be modified (if necessary) through information gathered by TGA and DTA analysis, in an effort to totally eliminate voids. Analysis by improved cross-sectional methods and instruments will be used.
  - 4. Tests to check the chemical durability of the composite bodies will be carried out.

#### REFERENCES

1. S. Sakka, K. Kama, J. Non-Cryst. Solids 42:403-422 (1980).
2. B.E. Yoldas, Applied Optics 21:16 (1982).
3. M. Nogami, Y. Moriya, J. Non-Cryst. Solids 37:191 (1979).
4. H. Verweig, G. DeWith, D. Veeneman, J. Mat. Sci. 20:1069 (1985).



END

DTIC

8-86